Genetics and Genomics

Dimeric ^{R25C}PTH(1-34) Activates the Parathyroid Hormone-1 Receptor *in vitro* and Stimulates Bone Formation in Osteoporotic Female Mice

Reviewed Preprint
v2 • December 13, 2024
Revised by authors

Reviewed Preprint
v1 • June 25, 2024

Minsoo Noh, Xiangguo Che, Xian Jin, Dong-Kyo Lee, Hyun-Ju Kim, Doo Ri Park, Soo Young Lee, Hunsang Lee, Thomas Gardella, Je-Yong Choi, Sihoon Lee

Department of Internal Medicine and Laboratory of Genomics and Translational Medicine, Gachon University College of Medicine, Incheon, Republic of Korea • Department of Life Sciences, Korea University, Seoul, Republic of Korea • Department of Biochemistry and Cell Biology, Cell and Matrix Research Institute, School of Medicine, Kyungpook National University, Daegu, Republic of Korea • Department of Life Sciences, Multitasking Macrophage Research Center, Ewha Womans University, Seoul, Republic of Korea • Endocrine Unit, Massachusetts General Hospital and Harvard Medical School, Boston, USA

https://en.wikipedia.org/wiki/Open_access
Copyright information

eLife Assessment

The study is noteworthy for its effort to achieve a deeper understanding of PTH-1 Receptor signaling. The PTH-1 pathway underpins the control of calcium and phosphate metabolism throughout life in land-dwelling animals and it can be targeted to therapeutic benefit in patients with osteoporosis. We consider the significance of the findings in this paper to be **valuable** to the community of investigators working on PTH receptor signaling, with **convincing** evidence.

https://doi.org/10.7554/eLife.97579.2.sa2

Abstract

Osteoporosis, characterized by reduced bone density and strength, increases fracture risk, pain, and limits mobility. Established therapies of Parathyroid hormone (PTH) analogs effectively promote bone formation and reduce fractures in severe osteoporosis, their use is limited by potential adverse effects. In the pursuit of safer osteoporosis treatments, we investigated ^{R25C}PTH, a PTH variant wherein the native arginine at position 25 is substituted by cysteine. These studies were prompted by our finding of high bone mineral density in a hypoparathyroidism patient with the R25C homozygous mutation, and we explored its effects on PTH type-1 receptor (PTH1R) signaling in cells and bone metabolism in mice. Our findings indicate that ^{R25C}PTH(1-84) forms dimers both intracellularly and extracellularly, and the synthetic dimeric peptide, ^{R25C}PTH(1-34), exhibits altered activity in PTH1R-mediated cAMP response. Upon a single injection in mice, dimeric ^{R25C}PTH(1-34) induced acute calcemic and phosphaturic responses comparable to PTH(1-34). Furthermore, repeated daily injections increased calvarial bone thickness in intact mice and improved trabecular and cortical bone parameters in ovariectomized (OVX) mice, akin to PTH(1-34). The overall results reveal a

capacity of a dimeric PTH peptide ligand to activate the PTH1R *in vitro* and *in vivo* as PTH, suggesting a potential path of therapeutic PTH analog development.

Introduction

Osteoporosis is a prevalent global bone disorder characterized by low bone mineral density (BMD), causing weakened bones prone leading to fragility fractures, particularly in the spine, hip, and wrist. The development of osteoporosis is influenced by factors including gender, being more prevalent in women; hormonal changes, like decreased estrogen levels during menopause; and age, with heightened susceptibility post-menopause in women contributing to bone loss. Recent meta- analysis of previous studies indicates a global osteoporosis prevalence of 23.1 % among women and 11.7 % among men (1, 2). Osteoporosis stands as a noteworthy risk factor that poses challenges to the preservation of autonomous mobility and overall well-being within an aging society. There is thus a pressing need for safe and efficacious therapies for osteoporosis that mitigate fractures, alleviate associated symptoms, and preserve physical functionality.

Anti-resorptive agents (e.g., bisphosphonates, denosumab, and romosozumab) encompass one therapeutic approach that aims to specifically counteract the declines in bone mass by tempering the balance between bone resorption and formation (3–5). It is pertinent to acknowledge, however, that the prolonged use of most of such agents is limited due to potential long-term side effects. Furthermore, most anti-resorptive therapies cannot stimulate new bone formation (6). In contrast, bone anabolic agents, such as parathyroid hormone (PTH) and its analogs, such as teriparatide (recombinant human PTH(1–34)), increase BMD by stimulating bone formation more than bone resorption (7). PTH has an exceptionally short half-life in the blood of approximately 2-4 minutes (8, 9), which helps in avoiding excessive increases in blood calcium levels that can otherwise limit the utility of PTH-related medications, while yet inducing a desired anabolic effect on bone. It is also worth noting that studies in rodents reveal that long-term administration of a PTH anabolic agent can lead to bone overgrowth, osteosarcoma, as well as hypercalcemia (10, 11). Consequently, a goal of ongoing research is to uncover the underlying molecular mechanisms driving the anabolic and catabolic effects of PTH to thereby secure more effective therapeutic alternatives for osteoporosis (12).

PTH is produced and secreted by the parathyroid glands as a straight-chain monomeric polypeptide of 84 amino acids (13–15). It plays a vital role in maintaining calcium and phosphate equilibrium by acting on the PTH1R, a class B G protein-coupled receptor (GPCR) (16–18) that is expressed primarily in cells of bone and kidney (19). The orchestrated downstream effects of PTH in target cells act to ensure optimal bone health and the maintenance of the ambient blood calcium and phosphate concentrations required for proper nerve conduction, muscle activity, and systemic cellular communication, whereas disturbances in this system can lead to multiple disorders.

Central to the PTH signaling cascade is the activation of intracellular G proteins (20), most prominently Gsα, which in turn activates transmembrane adenylyl cyclases, leading to the synthesis of the second messenger cyclic AMP (cAMP), and the activation of cAMP-dependent protein kinase A (PKA) (21, 22). PTH can also activate other second messenger cascades, including the Gαq/phospholipase C (PLC) / inositol 1,4,5-trisphosphate (IP3), diacylglycerol (DAG), and protein kinase C (PKC) signaling pathways (23, 24), highlighting the diverse biology of PTH and the PTH1R (25). Adding to this, the PTH1R also mediates the actions of parathyroid hormone-related protein (PTHrP), a development protein that acts in the formation of bones and other tissues. PTHrP shares homology with PTH in the first 34 amino acids, which encompass the receptor-binding portions of the two respective ligands. The PTH1R thus has an intrinsic capacity for dual ligand recognition, which opens possibilities for exploring new modes of therapeutic development for diseases such as osteoporosis and hypoparathyroidism (19, 20, 26–29).

Pharmacologically, the PTH1R can adopt at least two distinct ligand-binding conformations, RG and R^0, the selectivity for which can lead to altered modes of signaling *in vitro* and *in vivo* for peptides such as PTH, PTHrP, and various hybrid analogs (30–34) .

The current study extends our prior investigation in which we identified in a patient with chronic hypocalcemia and hyperphosphatemia a mutation that changes the arginine at position 25 in the mature PTH(1-84) polypeptide to cysteine (^{R25C}PTH) (35, 36). Antibody assays revealed the ^{R25C}PTH mutant protein to be present in the patient's blood at markedly elevated levels. We now have found that this patient expressing the ^{R25C}PTH variant has higher-than-normal BMD. We further characterize the ^{R25C}PTH protein and find that it can manifest in two distinct molecular forms: as a monomer and as a dimer, and we demonstrate that a dimeric ^{R25C}PTH(1-34) synthetic peptide retains agonistic properties on the PTH1R that are driven by a moderate selectivity for the RG vs. R^0 receptor conformation. Finally, we demonstrate in mice that ^{R25C}PTH(1-34) can induce skeletal responses that are similar to those induced by PTH(1–34), but without triggering an excessive hypercalcemic response. Considering the proven bone-anabolic capacity of several established PTH agonist ligands, and the need for safe, long-term treatments for skeletal disorders, our studies on dimeric ^{R25C}PTH(1- 34) suggest alternative strategies to consider in such drug development programs.

Results

Dimerization of ^{R25C}PTH(1-84)

In our previous studies, we showed that synthetic monomeric peptide, ^{R25C}PTH(1-34), as compared to PTH(1-34), exhibits a moderately diminished PTH1R-binding affinity and decreased cAMP signaling potency *in vitro*, and that with long-term infusion in mice, ^{R25C}PTH(1-34) leads to only minimal calcemic and phosphaturic effects, which corroborates the hypocalcemia seen in the original patient, despite the significantly elevated levels of ^{R25C}PTH in the plasma (35). In subsequent analysis of this patient, we found a particularly high BMD (Supplemental figure 1), which prompted us to further characterize the functional properties of ^{R25C}PTH, as described herein. We produced recombinant PTH(1-84) with or without the R25C mutation by expression of the corresponding cDNA in HEK293T cells (**Figure 1**). We considered the possibility that the introduction of a sole new cysteine within the polypeptide chain of ^{R25C}PTH(1-84) might induce homologous bimolecular dimerization through a disulfide bond involving the thiol functional group in each monomer (37, 38). To specifically investigate this, we designed the cDNA constructs to express either pre-pro-PTH(1-115)-3xFLAG or ^{R56C}pre-pro- PTH(1-115)-3xFLAG, such that after intracellular processing and cleavage of the pre-pro regions, the mature PTH(1-84)-3xFLAG or ^{R25C}PTH(1-84)-3xFLAG peptides would be generated upon transfection in HEK293T cells (**Figure 1C**) (39-41). We performed western blot analysis of total cell lysates and conditioned culture media collected from the transfected cells to specifically assess the possible presence of a disulfide-bonded dimeric form. Each sample was thus prepared in either reduced or non-reduced form and proteins were detected using an anti-flag antibody. The results demonstrated the presence of both a low molecular weight monomeric, and in the non-reduced samples, a higher molecular weight dimeric form of the ^{R25C}PTH(1-84)-3XFLAG protein in both the cell lysate and extracellular conditioned medium fractions, and the dimer appeared to be at an elevated proportion in the medium relative to the lysate (**Figure 1D**). To control for potential artifact effects attributed to the 3xFLAG tag, we utilized plasmid constructs pcDNA3.0-(pre-pro-PTH)-IRES and pcDNA3.0-(^{R56C}pre- pro-PTH)-IRES encoding non-tagged PTH variants and an anti-PTH(39-84) antibody for Western blot analysis, which again confirmed the presence of the dimer in total HEK293T cell lysates (Supplemental figure 2).

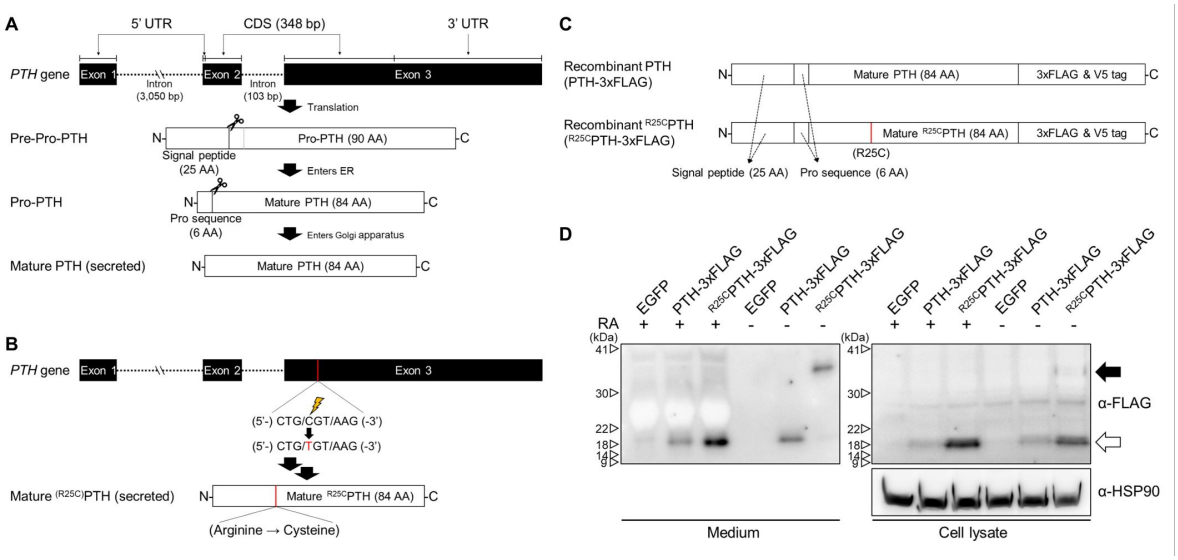

Figure 1.

Formation of R25C mutant PTH(1-84) dimer. (A) Schematic representation of PTH gene structure and expression. (B) Schematic representation of ^{R56C}pre-pro-PTH(1-115) (In mature form, ^{R25C}PTH(1-84)) gene structure and expression (C) Schematic representation of recombinant PTH proteins (D) *In vitro* dimerization of ^{R25C}PTH. Recombinant protein constructs were transfected into HEK293T cells, and expression of PTH-3xFLAG and ^{R25C}PTH3xFLAG in culture medium or cell lysate was demonstrated by western blot. The result confirms the presence of dimeric ^{R25C}PTH. (*bp: base pairs; *AA: amino acids; *RA: reducing agent)

We observed in the above studies that the expression level of ^{R25C}PTH(1-84) was higher than that of wild-type PTH(1-84) in both cell lysate and medium, which we considered might be due to an intrinsic enhancement in protein stability and resistance to protein degradation in the dimeric molecule. To address this, we treated the cells with the proteasome inhibitor MG132, which acts by forming a hemiacetal with the hydroxyl groups of active site threonine residues, and compared the expression levels of wild-type PTH(1-84) and ^{R25C}PTH(1-84) in the treated vs. untreated cells. The results indicated that while the expression level of wild-type PTH was increased by MG132 treatment, it did not reach the level of ^{R25C}PTH, suggesting that the difference in expression is not related to a difference in sensitivity to proteasome-mediated degradation (Supplemental figure 3).

Overall, we have confirmed that ^{R25C}PTH(1-84) can form a dimeric structure, and the ^{R25C}PTH(1-84) secreted outside the cells predominantly exists in dimeric form. Thus, utilizing dimer ^{R25C}PTH(1-84) in the analysis would be more relevant to understanding the actual function of ^{R25C}PTH.

Consequently, we aim to conduct further validation using dimeric ^{R25C}PTH in our subsequent investigations.

Functional characterization of dimeric ^{R25C}PTH(1-34) *in vitro*

To explore the functional properties of dimeric ^{R25C}PTH, we conducted experiments using synthetic peptides of PTH(1-34), ^{R25C}PTH(1-34) (monomeric) and disulfide-bonded dimeric ^{R25C}PTH(1- 34). First, we examined the receptor-binding affinity of these ligands by performing competition experiments using membranes prepared from HEK293-derived GP-2.3 cells that stably express the human PTH1R and assay formats designed to assess binding to either the G protein-uncoupled R^0 or G protein-coupled RG receptor conformation. The results revealed that monomeric ^{R25C}PTH(1-34) bound to both the R^0 and RG conformations with comparable, albeit slightly weaker affinity as compared to PTH(1-34), while dimeric ^{R25C}PTH(1-34) bound to each conformation with weaker affinity than did the monomeric form while showing an apparent selectivity for higher binding to the RG vs R^0 conformation of PTH1R (**Figure 2A**).

To investigate the signaling properties of the ligands, we measured the changes in the increase in intracellular levels of cAMP induced by each ligand in an osteoblastic SaOS-2 derived cell line (SGS-72 cells) that stably expresses the Glosensor cAMP reporter. These assays revealed that each ligand dose-dependently increased the cAMP levels in the cells, detected as an increase in luminescence in an Envision plate reader, and while the potencies were moderately and more substantially reduced for the monomeric and dimeric forms of the ligand, respectively, as compared to PTH(1-34), the maximum response attained by each ligand were comparable (**Figure 2B**). Dimeric ^{R25C}PTH(1-34) thus retains signaling functionality at the PTH1R that is characterized by a potency approximately commensurate with its affinity for binding to the RG PTH1R conformation.

Effect of single injection of dimeric ^{R25C}PTH(1-34) on calcium and phosphate regulation in mice

To assess whether dimeric ^{R25C}PTH can function *in vivo*, we injected the ligand, and in parallel either vehicle or PTH(1-34) (each peptide at a dose of 50 nmol/kg) into CD1 female mice and measured levels of ionized calcium (Ca^{2+}) in the blood (n = 6 mice/group), inorganic phosphate (Pi) in plasma (n = 12 mice/group), and the excretion of Pi into urine (n = 6 mice/group). Blood Ca^{2+} levels were measured at serial time points of pre-injection, 1, 2, 4, and 6 hours post-injection. Both PTH(1- 34) and dimeric ^{R25C}PTH(1-34) induced increases in blood Ca^{2+} levels that were significant, relative to the levels in vehicle-injected mice, at 1 and 2 hours post-injection, and the levels then returned to the baseline levels of vehicle control mice by 4 hours (**Figure 3A**). Plasma Pi levels were measured in samples obtained pre-injection, at 6 minutes, and 1, 2, and 6 hours post-

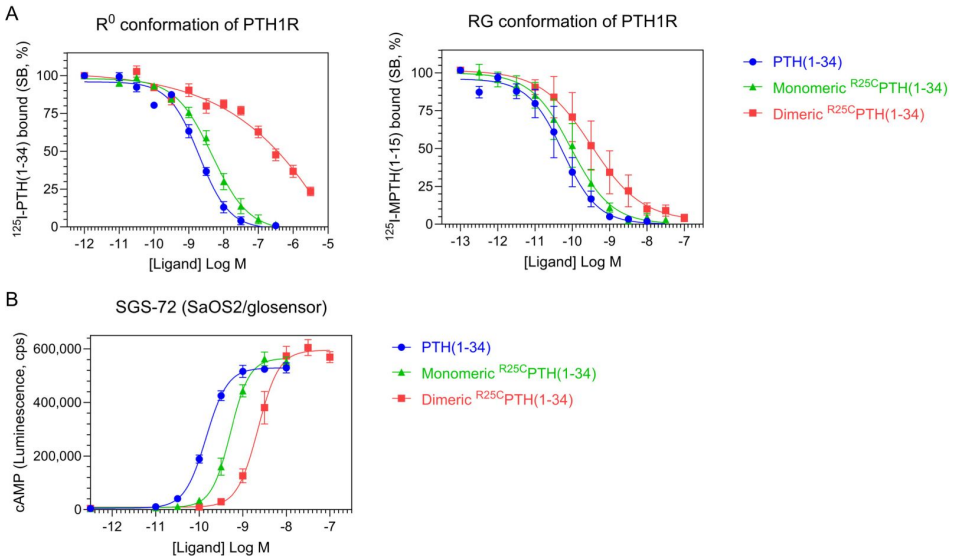

Figure 2.

Effect of PTH, monomeric ^{R25C}PTH, and dimeric ^{R25C}PTH to the PTH1R *in vitro*. (A) The binding of PTH(1-34), monomeric ^{R25C}PTH(1-34), and dimeric ^{R25C}PTH(1-34) to the PTH1R in R^0 conformation of RG conformation was assessed by competition methods using ^{125}I-PTH(1-34) and ^{125}I-MPTH(1-15) as radioligand (n = 4). (B) Ligand potency for cAMP signaling was assessed in SGS- 72 cells, which were derived from SaOS-2 cells modified to express Glosensor cAMP reporter (n = 4). The cells were preloaded with luciferin and treated with varying concentrations of PTH(1-34), monomeric ^{R25C}PTH(1-34), and dimeric ^{R25C}PTH(1-34). Error bars represent mean ± standard error.

injection. PTH(1-34) induced a significant decrease in plasma Pi at 1-hour post-injection, and the levels subsequently returned to baseline by 2 hours. Injection of dimeric ^{R25C}PTH(1-34) resulted in a slight decrease in plasma Pi at 2 hours post-injection, but the effect was not significant (**Figure 3B**). Consistent with this trend, Pi levels in the urine of mice injected with dimeric ^{R25C}PTH(1-34) were increased significantly at 2 hours post- injection and then gradually returned to baseline levels (**Figure 3C**). These results thus indicate that dimeric ^{R25C}PTH can elicit calcemic and phosphaturic responses *in vivo* that are fully with those expected for an injected PTH1R agonist ligand.

Effect of dimeric ^{R25C}PTH(1-34) on bone calvariae in mice

To initially assess the effects that short-term treatment of dimeric ^{R25C}PTH(1-34) can have on bone, we injected 8-week-old male C57BL/6 mice once a day for six days (days 1-6), with either dimeric ^{R25C}PTH(1-34), PTH(1-34) or vehicle, and after 10 days without treatment (day 16) followed by euthanasia, we isolated the calvariae for histological analysis of new bone formation. Specifically, we examined sections stained with hematoxylin and eosin (H&E) to assess the width of newly formed bone areas along the edge of each sample. These regions exhibited a more vivid coloration compared to the surrounding existing bone tissue, demarcated by a dotted line for clarity (**Figure 4A**). Measurements were taken below and above the dissection area where new bone had formed, and these measurements were then utilized to calculate the mean values for further analysis. These analyses revealed that both PTH(1-34) and dimeric ^{R25C}PTH(1-34) significantly increased the width of the new bone area by approximately four-fold, as compared to the vehicle group (**Figure 4B**). These findings thus support a capacity of dimeric ^{R25C}PTH(1-34) to induce new bone formation *in vivo,* similar to PTH, despite molecular and structural changes.

Effect of dimeric ^{R25C}PTH on bone mass in osteoporotic mice

To more directly assess the impact of dimeric ^{R25C}PTH(1-34) on bone mass, we administered it to ovariectomized (OVX) mice, which serve as a well-established model for postmenopausal osteoporosis. The OVX mice were injected 5 times per week for 4 weeks with either the dimeric ligand (OVX + dimeric ^{R25C}PTH(1-34), PTH(1-34) (OVX + PTH(1-34)) or vehicle (OVX + vehicle, OVX-controls), and sham-operated (Sham) mice were used as further controls. Mice were euthanized at the end of the injection period and tissue samples were isolated for analysis. Quantitative micro-computed tomography (μ-CT) analysis of the femurs obtained from each group revealed that, as compared to OVX + vehicle controls, treatment with PTH(1–34) increased femoral trabecular bone volume fraction (Tb.BV/TV) by 121%, cortical bone volume fraction (Ct.BV/TV) by 128%, cortical thickness (Ct.Th) by 115%, cortical area (Ct.Ar) by 110%, and cortical area fraction (Ct.Ar/Tt.Ar) by 118%, while decreased total tissue area (Tt.Ar) by 93% (**Figure 5A** and **5B**). Treatment with dimeric ^{R25C}PTH(1-34) had similar effects on the femoral cortical bone parameters, as it increased Ct.BMD by 104%, Ct.BV/TV by 125%, Ct.Th by 107%, and Ct.Ar/Tt.Ar by 116%, while decreased Tt.Ar 86% (**Figure 5**). Considering the reduction of Tt.Ar and no change of Ct.Ar compared to the OVX+vehicle controls, the increase of Ct.Ar/Tt.Ar indicates a decrease in bone marrow space. The increase in cortical bone BMD was significant with dimeric ^{R25C}PTH(1-34) but not with PTH(1-34), whereas an increase in femoral trabecular bone was only observed with PTH(1-34).

The effects of the treatments on bone strength were assessed by conducting a three-point bending test on femurs isolated from the mice. The maximum load parameter was significantly decreased in the femurs from OVX-control versus Sham mice and was significantly increased, relative to the OVX-controls, by treatment with the PTH(1-34), but not dimeric ^{R25C}PTH(1-34) (**Figure 5C**). The slope parameter was significantly decreased in the femurs from OVX-control versus Sham mice and tended to increase versus OVX-controls by treatment with either PTH(1-34) or ^{R25C}PTH(1-34), but the changes were not significant.

Figure 3.

Calcemic and phosphatemic responses by PTH injection in CD1 female mice. (A) Plasma Calcemic Response after Injection (n = 6). Both PTH(1-34) and dimeric ^{R25C}PTH(1-34) significantly elevate ionized calcium levels in plasma at 1 to 2 hours post-injection. After 2 hours post- injection, plasma ionized calcium level gradually restored to baseline levels similar to those of the vehicle group. (B) Plasma Phosphatemic Response after Injection (n = 12). Following PTH(1-34) injection, plasma phosphate levels significantly decrease at 1-hour post-injection, subsequently returning to baseline akin to those of the vehicle group. Conversely, dimeric ^{R25C}PTH(1-34) injection shows no significant alteration in phosphatemic response but demonstrates a tendency towards a slight decrease in phosphate levels, gradually restoring to baseline levels akin to those of the vehicle group. (C) Urine Phosphatemic Response after Injection (n = 6). The urine phosphate levels markedly increased at 1 hour post-injection for both PTH(1-34) and dimeric ^{R25C}PTH(1-34), followed by a return to baseline levels akin to those of the vehicle group. This analysis was conducted using 9-week-old female CD1 mice. The mice were administered PTH(1-34) and dimeric ^{R25C}PTH(1-34) at a concentration of 50 nmol/kg for each compound. Error bars represent mean ± standard error. *p*-values were determined using the two-way ANOVA to compare the mean of each test cell with the mean of the control cell at the same time point. * denotes *p*-value < 0.05 for PTH(1-34) compared to vehicle, ** denotes *p*-value < 0.01 for PTH(1-34) compared to vehicle, # denotes *p*-value < 0.05 for dimeric ^{R25C}PTH(1-34) compared to vehicle, ## denotes *p*-value < 0.01 for dimeric ^{R25C}PTH(1-34) compared to vehicle.

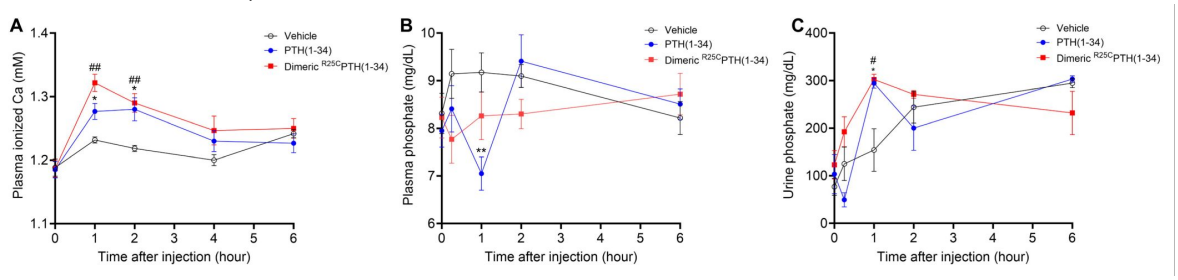

Figure 4.

Effect of dimeric ^{R25C}PTH(1-34) in calvarial injection model. (A) Dissections of the calvarial bones. Calvarial injections were performed on eight-week-old male C57BL/6 mice (N = 6 per group) that received daily administrations of vehicle, PTH(1-34), or dimeric ^{R25C}PTH(1-34) for six days. Following a 10-day treatment period, histological sections of calvariae, stained with hematoxylin (blue-purple; indicating cell nuclei) and eosin (pink; representing bone matrix), were obtained. The area of new bone formation, with more intense staining compared to the existing bone tissue, is denoted by the dotted line. The bar indicates 50 μm. (B) Quantification of new bone width in calvarial injection model. The result showed a significant increase in new bone width following injections of both PTH(1-34) and dimeric ^{R25C}PTH(1-34) compared to the vehicle group. *p*- values were obtained using the one-way ANOVA to compare the mean of each column with the mean of a control column. ** indicates *p*-value <0.01 against vehicle, *** indicates *p*-value <0.001 against vehicle.

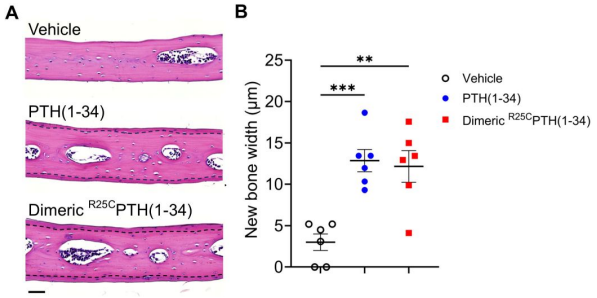

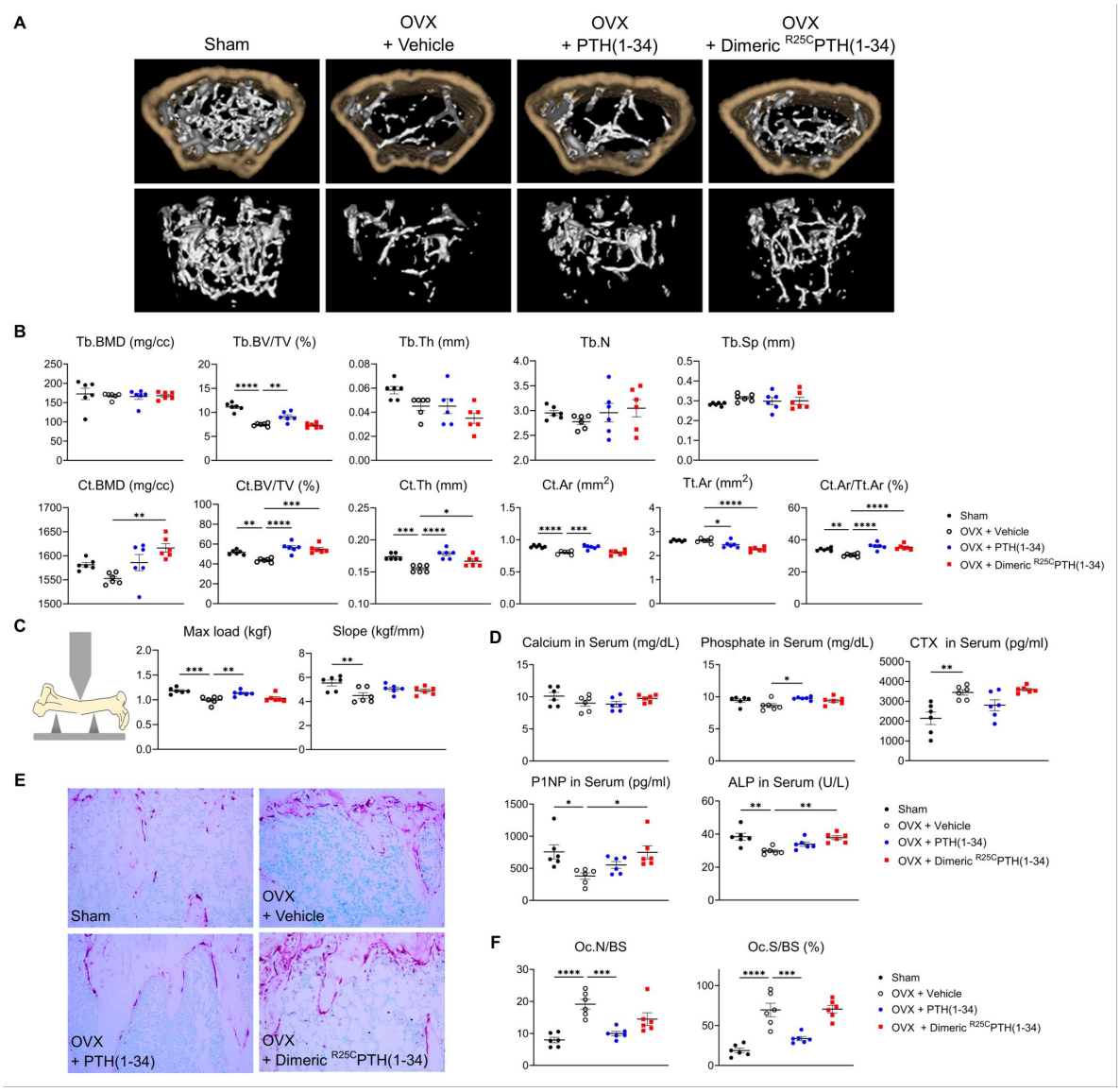

Figure 5.

Impact of ^{R25C}PTH(1-34) on Bone Turnover. The effects of Sham, OVX-Control (OVX + vehicle), OVX treated with PTH(1-34) (OVX + PTH(1-34)), and OVX treated with dimeric ^{R25C}PTH(1-34) (OVX + dimeric ^{R25C}PTH(1-34)) on bone turnover in mice. (A) Femurs obtained from mice in each group were subjected to μCT analyses for the assessment of bone mass. (B) Several parameters of (A) were quantified using μCT measurements, including trabecular bone mineral density (Tb.BMD), trabecular bone volume to tissue volume (Tb.BV/TV), trabecular bone thickness (Tb.Th), trabecular number (Tb.N), trabecular separation (Tb.Sp), cortical bone mineral density (Ct.BMD), cortical bone volume to tissue volume (Ct.BV/TV), cortical thickness (Ct.Th), cortical area (Ct.Ar), total tissue area (Tt.Ar), and cortical area to total tissue area (Ct.Ar/Tt.Ar). (C) A 3D-point bending test was conducted with femurs obtained from mice in each group. The left panel describes a schematic model of a 3D-point bending test. The middle and right panels each indicate the maximum bending load (kgf) and slope (kgf/mm). (D) Serum levels of calcium, phosphorus, CTX, P1NP, and ALP were measured for each group using an ELISA assay. (E) TRAP staining of histological sections of proximal tibias was carried out to visualize osteoclast activity. The scale bars represent 100 μm (F) Quantification of osteoclast number per bone surface (Oc.N/BS), and osteoclast surface per bone surface (Oc.S/BS) was performed. Each group consisted of six samples (n = 6). The error bars indicate mean ± standard error. *p*-values were obtained using the one-way ANOVA to compare the mean of each column with the mean of a control column. * indicates *p*-value < 0.05, ** indicates *p*-value < 0.01, *** indicates *p*-value < 0.001, **** indicates *p*-value < 0.0001.

We further analyzed the levels of bone metabolism markers in the serum obtained from the mice at the study endpoint (**Figure 5D**). The levels of serum calcium were within the normal range in all treatment groups, while serum phosphate levels were modestly increased in the OVX mice treated with PTH(1-34) or dimeric ^{R25C}PTH(1-34) as compared to with vehicle, but the effect was significant only with PTH(1-34). The serum levels of CTX-1, a bone resorption marker (42), were elevated in each of the OVX groups versus the Sham group, and tended to be lower in the OVX-PTH(1-34) treatment group, but the change relative to OVX-vehicle was not significant (**Figure 5D**). Interestingly, serum P1NP and alkaline phosphatase (ALP) levels were significantly increased in dimeric ^{R25C}PTH(1-34)-treated group, compared to the OVX-vehicle group (43, 44). Histological staining of proximal tibial sections for tartrate-resistant acid phosphatase (TRAP) activity, a marker of osteoclast- mediated bone resorption, revealed an apparent increase in this activity in bones of the OVX mice, as compared to those in Sham control mice, reflecting a heightened rate of bone turnover, as also suggested by the increased levels of serum CTX-1 in the OVX mice, and the TRAP staining appeared to be reduced in the tibiae of the OVX mice treated with PTH(1-34) (**Figure 5D and E**). Further histomorphometric analysis confirmed a significant increase in the osteoclast surface area relative to bone surface area (Oc.S/BS) in the proximal tibiae of the OVX-vehicle mice, relative to that in the Sham-control mice, and this parameter was significantly decreased by treatment with PTH(1-34), but not with dimeric ^{R25C}PTH(1-34) (**Figure 5F**).

We then analyzed the bone microstructure in the lumbar vertebrae through von Kossa staining of histological sections and histomorphometric quantification (**Figure 6A**). The trabecular bone volume fraction (Tb BV/TV, %), and trabecular number (Tb N) were significantly reduced in the OVX- vehicle group, as compared to the Sham group, and treatment with either PTH(1-34) or dimeric ^{R25C}PTH(1-34) resulted in a significant increase in each of these parameters, as well as a concomitant reduction in trabecular separation (Tb Sp), as compared to the respective parameters in the OVX- vehicle group (**Figure 6B**).

Dynamic bone histomorphometry was also performed on the vertebrae to evaluate rates of bone formation (**Figure 6C**). The trabecular mineral apposition rate (MAR) and cortical MAR were significantly increased in both the OVX-PTH(1-34) and OVX-dimeric ^{R25C}PTH(1-34) groups, as compared to in the OVX-vehicle group, and although there was a tendency for an increase in the bone formation rate (BFR/BS) in both the trabecular and cortical bone with either PTH(1-34) or dimeric ^{R25C}PTH(1-34) treatment, the differences were not statistically significant, as compared to the OVX control (**Figure 6D**).

In summary, injection of dimeric ^{R25C}PTH into osteoporotic OVX mice resulted in significant increases in cortical bone in the femurs and trabecular bone in the vertebrae, as well as significant increases in osteoblast function and serum markers of bone formation, ALP and P1NP, without inducing excessive bone resorption or hypercalcemia.

Discussion

In this study, we show the introduction of a cysteine mutation at the 25th amino acid position of mature parathyroid hormone (^{R25C}PTH) facilitates the formation of homodimers comprised of the resulting dimeric ^{R25C}PTH peptide *in vitro*. This dimerization surprisingly was compatible with receptor binding affinity and led to relatively minor deviations in functional behavior as assessed in our cell- based assays and compared to the standard monomeric control PTH peptide. The homozygous ^{R25C}PTH mutation was identified in patients who presented with hypocalcemia and hyperphosphatemia, despite elevated PTH levels (35, 45), and the mutation was found to impact the bioactive region of PTH (35, 46–49). Our initial research on this ^{R25C}PTH mutant focused on the monomeric state of the peptide, and these studies revealed relatively moderate decreases in PTH1R binding affinity and cAMP-stimulating potency *in vitro* and moderately

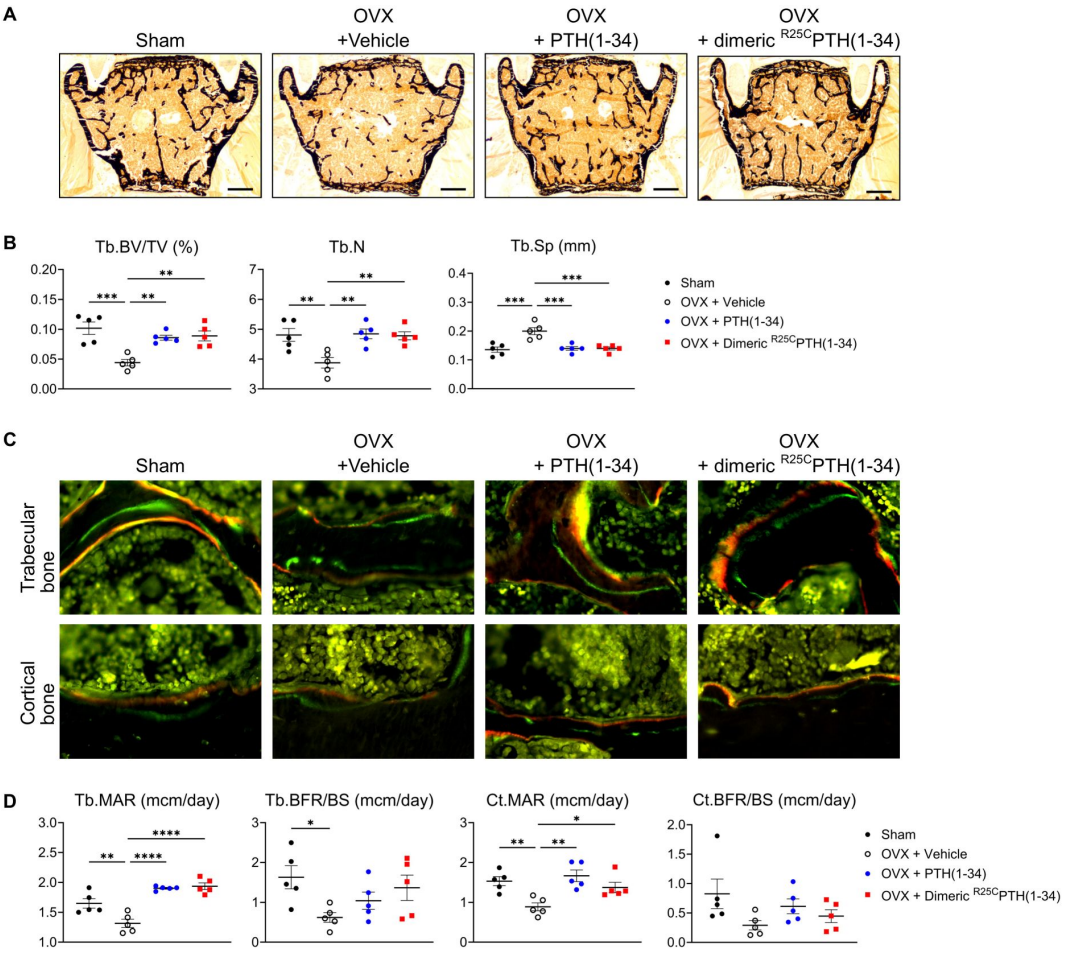

Figure 6.

Impact of ^{R25C}PTH(1-34) on Osteoblast Function in Vertebrae. The effects of Sham, OVX-Control (OVX + vehicle), OVX treated with PTH(1-34) (OVX + PTH(1-34)), and OVX treated with dimeric ^{R25C}PTH(1-34) (OVX + dimeric ^{R25C}PTH(1-34)) on osteoblast function in mice. (A) Mineralization of vertebrae obtained from each group was assessed through Von Kossa staining. (B) Quantification of trabecular bone parameters including trabecular bone volume to tissue volume (Tb.BV/TV), trabecular number (Tb.N), and trabecular separation (Tb.Sp) was performed using the Bioquant Osteo 2019 v19.9.60 program. Each bar represents 500 µm. (C) Fluorescent microscopic observations of trabecular and cortical bone sections from each group demonstrate the apposition of xylenol (red) and calcein (green) labels. (D) Quantification of trabecular bone parameters such as trabecular bone mineral apposition rate (Tb.MAR), trabecular bone formation rate to bone surface (Tb.BFR/BS), cortical bone MAR (Ct.MAR), and trabecular MAR (Tb.MAR) was carried out using the Bioquant Osteo 2019 v19.9.60 program. Each group consisted of five samples (n = 5). The error bars indicate mean ± standard error. *p*-values were obtained using the one-way ANOVA compare the mean of each column with the mean of a control column. * indicates *p*-value < 0.05, ** indicates *p*-value < 0.01, *** indicates *p*-value < 0.001, **** indicates *p*-value < 0.0001.

impaired calcemic effects upon infusion in mice. Additional patient observations, however, revealed the patients to have a higher BMD than anticipated for age-matched averages. This elevated bone mass, coupled with the elevated serum PTH levels, prompted our further investigations into the properties of the mutant PTH, as described herein.

Our investigations brought to light the capacity of the cysteine-25 mutation to induce dimer formation in the otherwise monomeric PTH polypeptide as produced in transfected cells. This result was established by comparing western blots of transfected cell lysates analyzed under reducing versus non-reducing conditions of gel electrophoresis. Subsequently, we employed synthetic peptides to further explore the functional properties of dimeric ^{R25C}PTH(1-34). The results of our current studies show some divergence from our previous findings obtained using the monomeric counterpart, ^{R25C}PTH (1-34) . Compared to the monomer, dimeric ^{R25C}PTH(1-34) exhibited a more preferential binding affinity for the RG versus R^0 PTH1R conformation, despite a diminished affinity for either conformation. We also observed that the potency of cAMP production in cells was lower for dimeric ^{R25C}PTH as compared to the monomeric ^{R25C}PTH, in accordance with a lower PTH1R-binding affinity. Previous reports indicated that a mutation at the 25th position of PTH results in the loss of calcium ion allosteric effects on monomeric ^{R25C}PTH, leading to faster ligand dissociation, rapid receptor recycling, and a shorter cAMP time course (50). Correspondingly, the weaker receptor affinity and reduced cAMP production observed in dimeric ^{R25C}PTH suggest a possibility that the formation of a disulfide bond at the 25th position significantly alters the function of PTH as a PTH1R ligand. While these structural effects are not yet fully understood and need to be investigated further.

We further pursued *in vivo* applications in mice. We assessed the calcemic and phosphatemic responses to a single injection of synthetic peptides of either PTH(1-34) or dimeric ^{R25C}PTH(1-34) in intact mice. We found the dimer could induce increases in plasma calcium levels that were at least as robust and as sustained as those induced by PTH(1-34) and were similarly phosphaturic (**Figure 3**).

Activation of the canonical Gαs-cAMP-PKA signaling pathway is generally thought to underly most of the biological responses induced by PTH1R activation, and our studies in SGS-72 cells confirm that dimeric PTH can activate this pathway, albeit not as efficiently as a monomeric PTH peptide. Arg25 resides in the 20-34 (C-terminal region) of PTH(1-34), which plays a significant role in the binding of the ligand to the extracellular domain (ECD) of the PTH1R. In concert with the binding of the 20-24 region of PTH to the ECD, the N-terminal portion of PTH engages the transmembrane domain (TMD) of the PTH1R, inducing the conformational changes involved in G protein coupling and cAMP production (34, 51–54). The precise binding mode used by dimeric ^{R25C}PTH to the PTH1R is unknown, but it may be anticipated that it differs to some extent from that used by the monomeric peptide, due, for example, to the changes in bulk molecular size and display of accessible functional groups. Consequently, the receptor conformational changes and the modes of coupling to downstream effectors may differ for the monomeric versus dimeric ligands, which could potentially lead to altered signaling and biological responses *in vivo*. Whether such changes account for the increased bone density observed in the patient with the homozygous ^{R25C}PTH mutation is unknown, but cannot be presently ruled out.

The results of practical assessments of dimeric ^{R25C}PTH(1-34) for effects on calvarial bone after short-term (6-days) injection into normal mice, and for effects on bone mass after long-term (4-weeks) daily injection in osteoporotic OVX mice demonstrate the dimer can mediate significant influences on bone metabolism alike to wild-type PTH. In OVX mice, PTH and dimeric ^{R25C}PTH significantly increased bone formation markers P1NP and ALP. However, wild-type PTH, but not dimeric ^{R25C}PTH, decreased bone resorption markers such as TRAP staining and CTX-1 levels, suggesting different effects of wild-type monomeric PTH and dimeric ^{R25C}PTH. In this study, the increase of bone resorption markers of dimeric ^{R25C}PTH compared to PTH may be one reason for low bone strength. While further investigation is necessary, the current experimental data, along

with patient symptoms showing no bone resorption despite lifelong exposure to high levels of ^{R25C}PTH, imply that the dimeric form of ^{R25C}PTH can provide a new insight into PTH and PTH analogs with distinct functionalities compared to the wild-type PTH.

This study has several limitations. First, it is urgently necessary to determine whether dimeric ^{R25C}PTH is present in human patient serum. Second, TRAP staining showed an inhibitory effect of PTH treatment on the primary spongiosa area. However, the secondary spongiosa, which more accurately reflects bone remodeling (55), was not examined due to the barely detectable bone in this area in OVX-induced osteoporosis mouse models. Third, it is unclear whether similar bone phenotypes exist between human ^{R25C}PTH patients and dimeric ^{R25C}PTH-treated mice, particularly regarding low bone strength. Although the dimeric ^{R25C}PTH-treated group showed higher cortical BMD compared to WT-Sham or PTH groups, there was no difference in bone strength compared to the osteoporotic mouse model. Fourth, our study showed that PTH or ^{R25C}PTH treatment decreased circumferential length; it is uncertain if this phenotype is also present in PTH-treated or ^{R25C}PTH patients. Finally, we did not analyze the ^{R25C}PTH mutant mouse model, which would allow us to compare phenotypes that most closely resemble those of human patients.

Interestingly, the recent identification of a young patient in Denmark displaying homozygous ^{R25C}PTH has opened avenues for observing the direct impacts of ^{R25C}PTH within the human biological system (45). The continual monitoring and observation of patients will contribute to a more profound comprehension of the long-term consequences associated with ^{R25C}PTH exposure. This extensive observation is crucial in delineating the extended effects of this compound on individuals. Consequently, by conducting thorough investigations to confirm the potential bone anabolic effect of ^{R25C}PTH, we hope to develop a novel bone anabolic agent with a targeted focus on the PTH1R.

Materials and methods

Plasmid construction

The coding sequences (CDS) of pre-pro-PTH and the mutated form, ^{R56C}pre-pro- PTH[^{R25C}PTH], were amplified using primers containing the attB site. These CDS fragments were obtained from pcDNA3.0-(hpre-pro-PTH)-IRES and pcDNA3.0-(h^{R56C}pre-pro-PTH)-IRES, which were used in the previous research conducted by Lee, *et al.* (35). Both CDS were introduced into donor vector pDONR223 with Gateway™ BP Clonase™ II Enzyme mix kit (Invitrogen, USA). Then pre-pro- PTH and ^{R56C}pre-pro-PTH were each cloned into pcDNA3.1-ccdB-3xFLAG-V5 with LR Gateway™ LR Clonase™ II Enzyme mix (Invitrogen, USA) to construct pcDNA3.1-(pre-pro-PTH)-3xFLAG-V5, and pcDNA3.1-(^{R56C}pre-pro-PTH)-3xFLAG-V5. All experimental procedures were done with the manufacturer's instruction. pDONR223 was a gift from Kim Lab (Roswell Park Comprehensive Cancer Center, USA), and pcDNA3.1-ccdB-3xFLAG-V5 was a gift from Taipale Lab (Donnelly Centre, University of Toronto, Canada).

Cell culture

All cell lines were grown at 37°C in 5 % CO_2. HEK293T cells were cultured in Dulbecco's Modified Eagle Medium (Cytiva™, HyClone DMEM/High glucose with L-Glutamine and HEPES, Cat No. SH30243.01, USA) with 10 % FBS (Gibco™, Fetal Bovine Serum, certified, Origin: USA, Cat No. 16000044, Lot No. 2522247RP, USA) and 1 % penicillin-streptomycin (Cytiva™, HyClone Penicillin-Streptomycin 100X solution, Cat No. SV30010, USA). Cell lines obtained from commercial sources were not further authenticated.

Transfection

pcDNA3.1-(pre-pro-PTH)-3xFLAG-V5 and pcDNA3.1-(^{R56C}pre-pro-PTH)-3xFLAG-V5 were each transfected into HEK293T with Lipofectamine™ 3000 Transfection Reagent (Invitrogen™, Cat No. L3000001, USA) according to the manufacturer's instruction. After 48 hours of transfection, a culture medium was collected and used for western blot as a secreted protein sample. The rest of the cells were lysed by RIPA buffer (Thermo Scientific™, RIPA Lysis and Extraction Buffer, Cat No. 89900, USA) following the manufacturer's instruction and used for western blot as total cell lysate sample.

Western blot

Protein samples were prepared in two types, reduced sample and non-reduced sample. Reduced samples were a mixture of protein (secreted protein or cell lysate), sample buffer (Invitrogen™, NuPAGE™ LDS Sample Buffer (4X), Cat No. NP0007, USA), with reducing agent (Invitrogen™, 10X Bolt™ Sample Reducing Agent, Cat No. B0009, USA) and heated for 5 min at 95°C. Non-reduced samples were a mixture of protein, and sample buffer, without reducing agent, and not heated. The protein samples were loaded onto 4 - 12 % Bis-Tris protein gels (GeneSTAR, StarPAGE Bis-Tris 4-12 %, 15-well, Cat No. GPG4115), and ran with MOPS/SDS running buffer (GeneSTAR, 20X MOPS/SDS Running Buffer, Cat No. GMB0080). Transfer to the membrane was done by iBlot™ 2 Dry Blotting System (Invitrogen™, iBlot™ 2 Gel Transfer Device, Cat No. IB21001, USA) with PVDF transfer stack (Invitrogen™, iBlot™ 2 Transfer Stacks-PVDF-mini, Cat No. IB24002, USA) according to manufacturer's instruction. The membranes were blocked for 1 hour at room temperature (RT) in 5 % skim-milk solution in Tris-buffered saline (TBS; 20 mM Tris-base, 500 mM NaCl, pH 7.5) and then washed three times for 10Jmin each with tris-buffered saline with 0.05 % tween-20 (TBST). The membranes were incubated with primary antibody for 1Jhour at RT, then washed three times for 10Jmin each with TBST. If needed, the membranes were incubated with horseradish peroxidase (HRP)-conjugated secondary antibody for 1 hour at RT after primary antibody incubation, then washed three times for 10Jmin each with TBST. After washing, the membranes were rinsed and soaked in TBS. To develop a blot image, the membranes were treated with a chemiluminescent substrate solution (Merck Millipore, Immobilon ECL Ultra Western HRP Substrate, Cat No. WBULS0500, USA) according to the manufacturer's instruction. The blot images were obtained by LAS 4000 mini (Cytiva, ImageQuant™ LAS 4000 mini, USA). The dilution condition for the anti-FLAG with hHRP conjugated antibody (Sigma-Aldrich, Monoclonal ANTI-FLAG® M2- Peroxidase (HRP) antibody produced in mouse, Cat No. A8592, USA) was 1:2,000. The dilution condition for the anti-HSP90 primary antibody (Santa Cruz Biotechnology Inc., HSP 90 Antibody (AC- 16), Cat No. sc-101494, USA) was 1:5,000. The dilution condition for the anti-mouse secondary antibody was 1:5,000. Each antibody was diluted in TBST with 1 % BSA solution.

Proteasome inhibition assay

HEK293T cells were seeded in culture dishes at approximately 60 % confluence, and they were allowed to grow for about 20 to 24 hours prior to transfection. The transfection of pcDNA3.1- (pre-pro-PTH)-3xFLAG-V5 and pcDNA3.1-(^{R56C}pre-pro-PTH)-3xFLAG-V5 was conducted following the method mentioned earlier. After 24 hours of transfection, MG132, dissolved in DMSO, was added to the cells to achieve a final concentration of 10 μM. For the mock treatment, DMSO alone was added. The cells were then incubated for an additional 24 hours after MG132 treatment. Both the culture medium and cell lysate were prepared for western blot analysis to assess the restored protein levels. The western blot procedure was carried out as described in the previous section.

Peptide synthesis and quantification

Human PTH(1-34), ^{R25C}PTH(1-34), and dimeric ^{R25C}PTH(1-34) were chemically synthesized by Anygen (Gwangju, Republic of Korea). The purity and mass of each peptide were analyzed by high-performance liquid chromatography (HPLC) and matrix-assisted laser desorption ionization-time

of flight mass spectrometry (MALDI-TOF MS) in the manufacturer.

PTH1R competition binding assay

The binding of PTH and its analogs to G protein-uncoupled PTH1R (R^0 conformation) and G protein-coupled PTH1R (RG conformation) was assessed using a competition method with membranes prepared from GP-2.3 cells (HEK-293 cells stably expressing the hPTH1R). For tracer radioligands, we utilized ^{125}I-PTH(1-34) and ^{125}I-MPTH(1-15). The unlabeled ligands tested were PTH(1–34), ^{R25C}PTH(1-34), and dimeric ^{R25C}PTH(1-34). Binding to the R^0 conformation was assessed using ^{125}I-PTH(1-34) as the tracer radioligand, while binding to the RG conformation was assessed using ^{125}I-MPTH(1-15). The addition of unlabeled ligands PTH(1–34), ^{R25C}PTH(1-34), or dimeric ^{R25C}PTH(1-34) caused dissociation of the tracer radioligand from each receptor if it had affinity to the receptors. Measurement of the dissociated ratio of the radioligand indicated the binding affinity between PTH1R and each unlabeled ligand. Each experiment was replicated four times.

cAMP assay

To measure intracellular cAMP production, SGS-72 cells, derived from SaOS-2 cells and stably expressing the Glosensor cAMP reporter, were utilized to measure intracellular cAMP production. The detection of cAMP-dependent expression was performed using an Envision plate reader (PerkinElmer, Waltham, MA, USA), based on luciferase-based luminescence, as previously described by Maeda, *et al.* (56). Each measurement was replicated four times.

Animal model used in the study

CD1 female mice were purchased from Charles River Laboratories (Massachusetts, USA), and all animal care and experimental procedures were conducted under the guidelines set by the Institutional Animal Care and Use Committee (IACUC) at Massachusetts General Hospital (MGH). The mice were housed in a specific pathogen-free environment, with 4-5 mice per cage, under a 12- hour light cycle at a temperature of 22±2°C.

Eight-week-old C57BL/6N female mice were purchased from KOATECH (Gyeonggi-do, Republic of Korea), and stabilized mice for 2 weeks. All animal care and experimental procedures were conducted under the guidelines set by the Institutional Animal Care and Use Committees of Kyungpook National University (KNU-2021-0101). The mice were housed in a specific pathogen-free environment, with 4-5 mice per cage, under a 12-h light cycle at 22 ± 2°C. They were provided with standard rodent chow and water ad libitum.

An ovariectomizing (OVX) osteoporosis mouse model was established using 10-week-old C57BL/6N female mice. Following surgery, mice were divided into the following four groups (n = 6 mice/group) as follows: Sham, OVX control group, OVX + PTH (1–34) treated group (40 μg/kg/day), and OVX + dimeric ^{R25C}PTH treated group (40-80 μg/kg/day). OVX mice were allowed to recover for 4 weeks after surgery. Afterward, PTH (1–34) or ^{R25C}PTH was injected subcutaneously 5 times a week for 4 weeks. Micro-computed tomography (μ-CT) and histological analyses were performed on 4 groups at 18 weeks of age.

Acute injections

The peptides PTH(1-34) and dimeric ^{R25C}PTH(1-34) were diluted in a solution comprising 0.05% Tween 80, 10 mM citric acid, and 150 mM NaCl at a pH of 5.0. Intravenous injections of these peptides were administered at doses ranging from 50-100 μg/kg into 9-week-old CD1 female mice. As a control, mice received only the vehicle. Levels of ionized calcium (Ca2+) in the blood (n = 6 mice/group) were measured at serial time points of pre-injection, 1, 2, 4, and 6 hours post-

injection. Inorganic phosphate (Pi) in plasma (n = 12 mice/group), and the excretion of Pi into urine (n = 6 mice/group) were measured in samples obtained at serial time points of pre-injection, at 6 minutes, and 1, 2, and 6 hours post-injection.

Calvarial injection mouse model

C57BL/6 male mice (8-week-old) were divided into the following three groups (n = 6 mice/group): control, PTH (1-34) treated group (80 μg/kg/day), and ^{R25C}PTH treated group (160 μg/kg/day). Subcutaneous injections of the respective drugs were administered once daily for 6 days. On the sixteenth day, the mice were sacrificed, and their bone tissues were harvested and fixed in 10 % formaldehyde at 4°C. The fixed bone tissues were then decalcified in PBS (pH 7.4) containing 0.5 moles of ethylenediaminetetraacetic acid (EDTA). Following decalcification, the tissues were embedded in paraffin, and paraffinized tissues were sectioned to a thickness of 5-7 μm. Histological analysis was performed using the sectioned tissue slides stained with hematoxylin and eosin (H&E). The area of new bone formation, which displays a more intense coloration compared to the existing bone tissue, was examined.

μ-CT analysis

Mouse femurs were fixed in a 4 % paraformaldehyde solution for 24 hours at 4°C. In μ-CT, we used the Quantum FX μ-CT (Perkin Elmer, Waltham, MA, USA). The images were acquired at a 9.7 μm voxel resolution, with settings of 90 kV and 200 μA, a 10 mm field of view, and a 3-minute exposure time. Serial cross-sectional images were reconstructed using the Analyze 12.0 software (Overland Park, KS, USA). To ensure consistent analysis, identical regions of interest (ROIs) were selected for the trabecular and cortical bones. Bone parameters and density were analyzed in the region between 0.3–1.755 mm (150 slices) from the bottom of the growth plate. Analysis of bone structure was performed using adaptive thresholding in CT Analyser. Thresholds for analysis were determined manually based on grayscale values for each experimental group: trabecular bone: 3000; cortical bone: 5000 for all samples. All bone parameters were evaluated according to the guidelines of the American Society for Bone and Mineral Research (57).

Three-point bending test

The left femur of the mouse was immersed in 0.9 % NaCl solution, wrapped in gauze, and stored at −20°C until ready for a three-point bending test. In this test, we placed the mouse femurs horizontally with the anterior surface facing upwards, centered on the supports, and the compressive force was applied vertically to the mid-shaft. The pressure sensor was positioned at a distance that allowed maximum allowable pressure (200N) without interfering with the test (20.0 mm for the femur). A miniature material testing machine (Instron, MA, U.S.A.) was used for this test. The crosshead speed was decreased to 1 mm/min until failure. During the test, force-displacement data were collected to determine the maximum load and slope of the bones.

Serum biochemistry analysis

Serum bone resorption and osteogenesis marker levels, specifically the C-terminal telopeptide of type I collagen (CTX) and procollagen type I N-terminal propeptide (P1NP), were assessed in mice from the Sham, OVX-control, PTH(1-34), and dimeric ^{R25C}PTH(1-34) groups by using the enzyme-linked immunosorbent assay (ELISA) according to the manufacturer's instructions. Additionally, their concentrations were determined using specific mouse CTX-1 and P1NP ELISA kits (Cloud Clone, Wuhan, China) respectively.

Bone histological analyses

The tibiae were initially fixed in 4% paraformaldehyde at 4°C overnight. The following day, samples were decalcified using 10% ethylenediaminetetraacetic acid (EDTA) solution (pH 7.4) for 4 weeks at 4°C. The decalcified tibiae were then embedded in paraffin and sectioned at 3 μm thick.

For TRAP staining, dehydrated paraffin sections were fixed in an acetone/ethanol mixture (1:1) for 1 minute, followed by complete air-drying at RT for 20 minutes. Thereafter, the sections were immersed in TRAP reagent for 30 minutes at 37°C. In the histomorphometry analysis for TRAP staining, we used the primary spongiosa for the trabecular ROI because of the barely detectable in the secondary spongiosa of OVX model. Osteoclast surface per bone surface (Oc.S/BS) and Osteoclast number per bone surface (Oc.N/BS) analysis followed the ASBMR guidelines (58).

Dynamic bone histomorphometric analysis

To conduct dynamic histomorphometry analysis, we injected the mice with 25 mg/kg body weight of calcein (Sigma-Aldrich) or Alizarin Red S (Sigma-Aldrich) intraperitoneally before sacrifice, with 3- or 10-day intervals between injections as previously described (59, 60). Briefly, femurs or vertebrates were fixed in 4 % paraformaldehyde solution for 24 hours at 4°C. The following day, the samples were washed with phosphate-buffered saline (PBS) solution and then dehydrated using a gradient of ethanol (50 %, 70 %, 85 %, 90 %, and 100 %). Subsequently, we embedded the dehydrated femurs or vertebrates in methyl methacrylate (Sigma) to prepare resin blocks. The resin blocks were sectioned at 6 μm thick by using a Leica SP1600 microtome (Leica Microsystems, Germany). The fluorescence signals of calcein (green) and Alizarin Red S (red) from ROIs were captured using a fluorescence microscope (Leica, Wetzlar, Germany). For vertebral bone analysis, bone mineralization was evaluated by von Kossa staining. The sections were placed in 2-methoxyethyl acetate (Sigma-Aldrich) for 20 minutes, followed by rehydration with serial ethanol solutions (100 %, 90 %, 80 %, 70 %, and 50 %) and distilled water for 2 minutes each. The sections were subsequently dipped in a 1 % $AgNO_3$ solution (Sigma-Aldrich) for 5 minutes under ultraviolet (UV) light photons, washed in distilled water for 5 minutes, and dipped in 5 % sodium thiosulfate solution for 5 minutes to remove nonspecific binding. Finally, we covered the sections with mounting solution and captured images by using a Leica microscope. The parameters of dynamic bone histomorphometry were analyzed using the Bioquant Osteo 2019ME program (Bioquant Osteo, Nashville, TN, USA).

Statistical analysis

Statistical analysis was performed in GraphPad Prism 10.1.2. The data are presented as the mean ± standard error of the means (SEM). Statistically significant differences between the two groups were determined using an analysis of variance (ANOVA). A *p*-value less than 0.05 was considered statistically significant.

Author contributions

Conceptualization, Methodology: M.N., X.C., X.J., D-K.L., H-J.K., D.P., S.Y.L., H.L., T.J.G., J.-Y.C., and S.L.; Validation, Formal Analysis: M.N., and X.C.; Investigation, Resource: M.N., X.C., X.J., D.- K.L., and D.P.; writing - Original Draft Preparation: M.N., and X.C.; Writing – Review & Editing: M.N., X.C., T.J.G., H.L., J.-Y.C., and S.L.; Visualization: M.N., and X.C.; Supervision: H.-J.K., H.L., J.-Y.C., and S.L.; Project Administration: J.-Y.C., and S.L.; Funding Acquisition: S.Y.L., H.L., J.-Y.C., and S.L.

Acknowledgements

This work was supported by the National Research Foundation of Korea (NRF) grant funded by the Korea government (MSIT) (2022R1A2C3006002 to S.L.; 2022R1F1A1074610 and 2022R1A4A1025913 to H.L.; RS-2023-00217798 and 2021R1A2C3003675 S.Y.L.; 2022R1A2C1006105 to J.-Y.C.), Gachon University Gil Medical Center (FRD2023-12 to S.L.), and Korea University Grants.

References

1. Sozen T., Ozisik L., Basaran N. C. (2017) **An overview and management of osteoporosis** *Eur J Rheumatol* **4**:46–56

2. Salari N., et al. (2021) **The global prevalence of osteoporosis in the world: a comprehensive systematic review and meta-analysis** *J Orthop Surg Res* **16**

3. Papapoulos S., et al. (2012) **Five years of denosumab exposure in women with postmenopausal osteoporosis: results from the first two years of the FREEDOM extension** *J Bone Miner Res* **27**:694–701

4. Reid D. M., et al. (2009) **Zoledronic acid and risedronate in the prevention and treatment of glucocorticoid-induced osteoporosis (HORIZON): a multicentre, double-blind, double-dummy, randomised controlled trial** *Lancet* **373**:1253–1263

5. McClung M. R., et al. (2014) **Romosozumab in postmenopausal women with low bone mineral density** *N Engl J Med* **370**:412–420

6. Cosman F., et al. (2016) **Romosozumab Treatment in Postmenopausal Women with Osteoporosis** *N Engl J Med* **375**:1532–1543

7. Martin T. J., Sims N. A., Seeman E. (2021) **Physiological and pharmacological roles of PTH and PTHrP in bone using their shared receptor, PTH1R** *Endocrine reviews* **42**

8. Bieglmayer C., Prager G., Niederle B. (2002) **Kinetic analyses of parathyroid hormone clearance as measured by three rapid immunoassays during parathyroidectomy** *Clinical Chemistry* **48**:1731–1738

9. Maier G. W., et al. (1998) **Parathyroid hormone after adenectomy for primary hyperparathyroidism. A study of peptide hormone elimination kinetics in humans** *J Clin Endocrinol Metab* **83**:3852–3856

10. Vahle J. L., et al. (2002) **Skeletal changes in rats given daily subcutaneous injections of recombinant human parathyroid hormone (1-34) for 2 years and relevance to human safety** *Toxicol Pathol* **30**:312–321

11. Appelman-Dijkstra N. M., Papapoulos S. E. (2016) **From disease to treatment: from rare skeletal disorders to treatments for osteoporosis** *Endocrine* **52**:414–426

12. Khosla S., Hofbauer L. C. (2017) **Osteoporosis treatment: recent developments and ongoing challenges** *Lancet Diabetes Endocrinol* **5**:898–907

13. Moallem E., Kilav R., Silver J., Naveh-Many T. (1998) **RNA-Protein binding and post-transcriptional regulation of parathyroid hormone gene expression by calcium and phosphate** *J Biol Chem* **273**:5253–5259

14. Silver J., Russell J., Sherwood L. M. (1985) **Regulation by vitamin D metabolites of messenger ribonucleic acid for preproparathyroid hormone in isolated bovine parathyroid cells** *Proc Natl Acad Sci U S A* **82**:4270–4273

15. Chen R. A., Goodman W. G. (2004) **Role of the calcium-sensing receptor in parathyroid gland physiology** *Am J Physiol Renal Physiol* **286**:F1005–1011

16. Habener J. F., Rosenblatt M., Potts J. T. (1984) **Parathyroid hormone: biochemical aspects of biosynthesis, secretion, action, and metabolism** *Physiol Rev* **64**:985–1053

17. Veldurthy V., et al. (2016) **Vitamin D, calcium homeostasis and aging** *Bone Res* **4**

18. Kiela P. R., Ghishan F. K. (2009) **Recent advances in the renal-skeletal-gut axis that controls phosphate homeostasis** *Lab Invest* **89**:7–14

19. Jüppner H., et al. (1991) **AG protein-linked receptor for parathyroid hormone and parathyroid hormone-related peptide** *Science* **254**:1024–1026

20. Gardella T. J., Jüppner H. (2000) **Interaction of PTH and PTHrP with their receptors** *Reviews in Endocrine and Metabolic Disorders* **1**:317–329

21. Weinstein L. S., Yu S., Warner D. R., Liu J. (2001) **Endocrine manifestations of stimulatory G protein alpha-subunit mutations and the role of genomic imprinting** *Endocr Rev* **22**:675–705

22. Feinstein T. N., et al. (2011) **Retromer terminates the generation of cAMP by internalized PTH receptors** *Nat Chem Biol* **7**:278–284

23. Iida-Klein A., et al. (1997) **Mutations in the second cytoplasmic loop of the rat parathyroid hormone (PTH)/PTH-related protein receptor result in selective loss of PTH-stimulated phospholipase C activity** *J Biol Chem* **272**:6882–6889

24. Dunlay R., Hruska K. (1990) **PTH receptor coupling to phospholipase C is an alternate pathway of signal transduction in bone and kidney** *Am J Physiol* **258**:F223–231

25. Abou-Samra A.-B., et al. (1992) **Expression cloning of a common receptor for parathyroid hormone and parathyroid hormone-related peptide from rat osteoblast-like cells: a single receptor stimulates intracellular accumulation of both cAMP and inositol trisphosphates and increases intracellular free calcium** *Proceedings of the National Academy of Sciences* **89**:2732–2736

26. Bone H. G., et al. (2004) **Ten years' experience with alendronate for osteoporosis in postmenopausal women** *N Engl J Med* **350**:1189–1199

27. Rubin M. R., et al. (2016) **Therapy of Hypoparathyroidism With PTH(1-84): A Prospective Six Year Investigation of Efficacy and Safety** *J Clin Endocrinol Metab* **101**:2742–2750

28. Winer K. K., Yanovski J. A., Cutler G. B. (1996) **Synthetic human parathyroid hormone 1-34 vs calcitriol and calcium in the treatment of hypoparathyroidism** *JAMA* **276**:631–636

29. Winer K. K., et al. (2018) **Long-Term Parathyroid Hormone 1-34 Replacement Therapy in Children with Hypoparathyroidism** *J Pediatr* **203**:391–399

30. Okazaki M., et al. (2008) **Prolonged signaling at the parathyroid hormone receptor by peptide ligands targeted to a specific receptor conformation** *Proceedings of the National Academy of Sciences* **105**:16525–16530

31. Pioszak A. A., Parker N. R., Gardella T. J., Xu H. E. (2009) **Structural basis for parathyroid hormone- related protein binding to the parathyroid hormone receptor and design of conformation- selective peptides** *J Biol Chem* **284**:28382–28391

32. Cheloha R. W., Gellman S. H., Vilardaga J. P., Gardella T. J. (2015) **PTH receptor-1 signalling-mechanistic insights and therapeutic prospects** *Nat Rev Endocrinol* **11**:712–724

33. Hoare S. R., Gardella T. J., Usdin T. B. (2001) **Evaluating the signal transduction mechanism of the parathyroid hormone 1 receptor. Effect of receptor-G-protein interaction on the ligand binding mechanism and receptor conformation** *J Biol Chem* **276**:7741–7753

34. Dean T., Vilardaga J. P., Potts J. T., Gardella T. J. (2008) **Altered selectivity of parathyroid hormone (PTH) and PTH-related protein (PTHrP) for distinct conformations of the PTH/PTHrP receptor** *Mol Endocrinol* **22**:156–166

35. Lee S., et al. (2015) **A Homozygous [Cys25]PTH(1-84) Mutation That Impairs PTH/PTHrP Receptor Activation Defines a Novel Form of Hypoparathyroidism** *J Bone Miner Res* **30**:1803–1813

36. Bae C. H., et al. (2016) **A novel human PTH analog [Cys25] hPTH (1–34) restores bone mass in ovariectomized mice** *The Journal of Clinical Endocrinology & Metabolism* **101**:3700–3708

37. Banerjee R. R., Lazar M. A. (2001) **Dimerization of resistin and resistin-like molecules is determined by a single cysteine** *J Biol Chem* **276**:25970–25973

38. Trivedi M. V., Laurence J. S., Siahaan T. J. (2009) **The role of thiols and disulfides on protein stability** *Curr Protein Pept Sci* **10**:614–625

39. Kemper B., Habener J. F., Mulligan R. C., Potts J. T., Rich A. (1974) **Pre-proparathyroid hormone: a direct translation product of parathyroid messenger RNA** *Proc Natl Acad Sci U S A* **71**:3731–3735

40. Vasicek T. J., et al. (1983) **Nucleotide sequence of the human parathyroid hormone gene** *Proc Natl Acad Sci U S A* **80**:2127–2131

41. Wiren K. M., et al. (1989) **Mutations in signal sequence cleavage domain of preproparathyroid hormone alter protein translocation, signal sequence cleavage, and membrane-binding properties** *Mol Endocrinol* **3**:240–250

42. Rosen H. N., et al. (2000) **Serum CTX: a new marker of bone resorption that shows treatment effect more often than other markers because of low coefficient of variability and large changes with bisphosphonate therapy** *Calcif Tissue Int* **66**:100–103

43. Pagani F., Francucci C. M., Moro L. (2005) **Markers of bone turnover: biochemical and clinical perspectives** *J Endocrinol Invest* **28**:8–13

44. Wheater G., Elshahaly M., Tuck S. P., Datta H. K., van Laar J. M. (2013) **The clinical utility of bone marker measurements in osteoporosis** *J Transl Med* **11**

45. Andersen S. L., Frederiksen A. L., Rasmussen A. B., Madsen M., Christensen A. R. (2022) **Homozygous missense variant of PTH (c.166C>T, p.(Arg56Cys)) as the cause of familial isolated hypoparathyroidism in a three-year-old child** *J Pediatr Endocrinol Metab* **35**

46. Arnold A., et al. (1990) **Mutation of the signal peptide-encoding region of the preproparathyroid hormone gene in familial isolated hypoparathyroidism** *J Clin Invest* **86**:1084–1087

47. Parkinson D. B., Thakker R. V. (1992) **A donor splice site mutation in the parathyroid hormone gene is associated with autosomal recessive hypoparathyroidism** *Nat Genet* **1**:149–152

48. Sunthornthepvarakul T., Churesigaew S., Ngowngarmratana S. (1999) **A novel mutation of the signal peptide of the preproparathyroid hormone gene associated with autosomal recessive familial isolated hypoparathyroidism** *J Clin Endocrinol Metab* **84**:3792–3796

49. Ertl D. A., Stary S., Streubel B., Raimann A., Haeusler G. (2012) **A novel homozygous mutation in the parathyroid hormone gene (PTH) in a girl with isolated hypoparathyroidism** *Bone* **51**:629–632

50. White A. D., et al. (2019) **Ca(2+) allostery in PTH-receptor signaling** *Proc Natl Acad Sci U S A* **116**:3294–3299

51. Clark L. J., et al. (2020) **Allosteric interactions in the parathyroid hormone GPCR-arrestin complex formation** *Nat Chem Biol* **16**:1096–1104

52. Kumar A., Baumann M., Balbach J. (2016) **Small Molecule Inhibited Parathyroid Hormone Mediated cAMP Response by N-Terminal Peptide Binding** *Sci Rep* **6**

53. Zhao L. H., et al. (2019) **Structure and dynamics of the active human parathyroid hormone receptor-1** *Science* **364**:148–153

54. Zhai X., et al. (2022) **Molecular insights into the distinct signaling duration for the peptide-induced PTH1R activation** *Nat Commun* **13**

55. Jilka R. L. (2007) **Molecular and cellular mechanisms of the anabolic effect of intermittent PTH** *Bone* **40**:1434–1446

56. Maeda A., et al. (2013) **Critical role of parathyroid hormone (PTH) receptor-1 phosphorylation in regulating acute responses to PTH** *Proc Natl Acad Sci U S A* **110**:5864–5869

57. Bouxsein M. L., et al. (2010) **Guidelines for assessment of bone microstructure in rodents using micro-computed tomography** *J Bone Miner Res* **25**:1468–1486

58. Dempster D. W., et al. (2013) **Standardized nomenclature, symbols, and units for bone histomorphometry: a 2012 update of the report of the ASBMR Histomorphometry Nomenclature Committee** *J Bone Miner Res* **28**:2–17

59. Lim K. E., et al. (2015) **Core binding factor β of osteoblasts maintains cortical bone mass via stabilization of Runx2 in mice** *Journal of Bone and Mineral Research* **30**:715–722

60. Jin X., et al. (2024) **Silk sericin-based functional food for osteoporosis prevention and therapy** *Journal of Functional Foods* **116**

Author information

Minsoo Noh*

Department of Internal Medicine and Laboratory of Genomics and Translational Medicine, Gachon University College of Medicine, Incheon, Republic of Korea, Department of Life Sciences, Korea University, Seoul, Republic of Korea
ORCID iD: 0000-0002-1239-3783

*These two authors are equally contributed to this manuscript.

Xiangguo Che*

Department of Biochemistry and Cell Biology, Cell and Matrix Research Institute, School of Medicine, Kyungpook National University, Daegu, Republic of Korea

*These two authors are equally contributed to this manuscript.

Xian Jin

Department of Biochemistry and Cell Biology, Cell and Matrix Research Institute, School of Medicine, Kyungpook National University, Daegu, Republic of Korea

Dong-Kyo Lee

Department of Biochemistry and Cell Biology, Cell and Matrix Research Institute, School of Medicine, Kyungpook National University, Daegu, Republic of Korea

Hyun-Ju Kim

Department of Biochemistry and Cell Biology, Cell and Matrix Research Institute, School of Medicine, Kyungpook National University, Daegu, Republic of Korea

Doo Ri Park

Department of Life Sciences, Multitasking Macrophage Research Center, Ewha Womans University, Seoul, Republic of Korea

Soo Young Lee

Department of Life Sciences, Multitasking Macrophage Research Center, Ewha Womans University, Seoul, Republic of Korea

Hunsang Lee

Department of Life Sciences, Korea University, Seoul, Republic of Korea

Thomas Gardella

Endocrine Unit, Massachusetts General Hospital and Harvard Medical School, Boston, USA

Je-Yong Choi

Department of Biochemistry and Cell Biology, Cell and Matrix Research Institute, School of Medicine, Kyungpook National University, Daegu, Republic of Korea

For correspondence: jechoi@knu.ac.kr

Sihoon Lee
Department of Internal Medicine and Laboratory of Genomics and Translational Medicine, Gachon University College of Medicine, Incheon, Republic of Korea
ORCID iD: 0000-0002-9444-5849

For correspondence: shleemd@gachon.ac.kr

Editors

Reviewing Editor
Dolores Shoback
University of California, San Francisco, San Francisco, United States of America

Senior Editor
Dolores Shoback
University of California, San Francisco, San Francisco, United States of America

Reviewer #1 (Public review):

Summary:

In this work, the authors investigate the functional difference between the most commonly expressed form of PTH, and a novel point mutation in PTH identified in a patient with chronic hypocalcemia and hyperphosphatemia. The value of this mutant form of PTH as a potential anabolic agent for bone is investigated alongside PTH(1-84), which is a current anabolic therapy. The authors have achieved the aims of the study. Their conclusion that this suggests a "new path of therapeutic PTH analog development" seems unfounded; the benefit of this PTH variant is not clear, but the work is still interesting.

The work does not identify why the patient with this mutation has hypocalcemia and hyperphosphatemia; this was not the goal of the study, but the data is useful for helping to understand it.

Strengths:

The work is novel, as it describes the function of a novel, naturally occurring, variant of PTH in terms of its ability to dimerise, to lead to cAMP activation, to increase serum calcium, and its pharmacological action compared to normal PTH.

Weaknesses:

(1) The use of very young, 10 week old, mice as a model of postmenopausal osteoporosis remains a limitation of this study, but this is now quite clearly described as a limitation,, including justifying the use of the primary spongiosa as a measurement site.

(2) Methods have been clarified. It is still necessary to properly define the micro-CT threshold in mm HA/cc^3. I think it might be at about 200mg HA/cc^3 in this study.

(3) The apparent contradiction between the cortical thickness data (where there is no difference between the two PTH formulations) and the mechanical testing data (where there is a difference) remains unresolved. It is still not clear whether there is a material defect in the bone, which can be partially assessed by reporting the 3 point bending test, corrected for the diameters of the bone (i.e. as stress / strain curves).

(4) It is also puzzling that both dimeric and monomeric PTH lead to a reduction in total bone area (cross sectional area?). This would suggest a reduction in bone growth. This should be discussed in the work.

https://doi.org/10.7554/eLife.97579.2.sa1

Author response:

The following is the authors' response to the original reviews.

> ***Public Reviews:***
>
> ***Reviewer #1 (Public Review):***
>
> *Summary:*
>
> *In this work, the authors investigate the functional difference between the most commonly expressed form of PTH, and a novel point mutation in PTH identified in a patient with chronic hypocalcemia and hyperphosphatemia. The value of this mutant form of PTH as a potential anabolic agent for bone is investigated alongside PTH(1-84), which is a previously used anabolic therapy. The authors have achieved the aims of the study. Their conclusion, however, that this suggests a "new path of therapeutic PTH analog development" seems unfounded; the benefit of this PTH variant is not clear, but the work is still interesting.*
>
> *The work does not identify why the patient with this mutation has hypocalcemia and hyperphosphatemia; this was not the goal of the study, but the data are useful for helping to understand that.*
>
> *Strengths:*
>
> *The work is novel, as it describes the function of a novel, naturally occurring, variant of PTH in terms of its ability to dimerise, to lead to cAMP activation, to increase serum calcium, and its pharmacological action compared to normal PTH.*
>
> *Weaknesses:*
>
> *(1) The use of very young, 8-10 week old, mice as a model of postmenopausal osteoporosis is a major limitation of this study. At 8 weeks, the effect of ovariectomy leads to lack of new trabecular bone formation, rather than trabecular bone loss due to a defect in bone remodelling. Although the findings here provide a comparison between two forms of PTH, it is unlikely to be of direct relevance to the patient population. For example, the authors find an inhibitory effect of PTH on osteoclast surface, which is very unusual. Adding to this concern is that the authors have not described the regions used for histomorphometry, and from their figures (particularly the TRAP stain), it seems that the primary spongiosa (which is a region of growth) has been used for histomorphometry, rather than the secondary spongiosa (which more accurately reflects bone remodelling). Much further detail is needed to justify the use of this very young model, and a section on the limitations of this model is needed. Please provide that section in the revised manuscript.*

Thank you for your crucial comment. We obtained 8-week-old female mice and stabilized them in our facility for 2 weeks. Then, we performed OVX using 10-week-old mice and determined the effects of dimeric ^{R25C}PTH(1-34) on bone after 8 weeks because of 4 weeks for recovery and 4 weeks for PTH or ^{R25C}PTH(1-34). Therefore, we sacrificed the mice at 18-week-

old mice. We revised the method section on page 18, line 436-441 and page 18, line 442-448 as follows.

- 'Eight-week-old C57BL/6N female mice were purchased from KOATECH (Gyeonggi-do, Republic of Korea), and stabilized mice for 2 weeks. All animal care and experimental procedures were conducted under the guidelines set by the Institutional Animal Care and Use Committees of Kyungpook National University (KNU-2021-0101). The mice were housed in a specific pathogen-free environment, with 4-5 mice per cage, under a 12-h light cycle at 22 ± 2°C. They were provided with standard rodent chow and water *ad libitum*.'

- 'An ovariectomized (OVX) mouse model was established using 10-week-old C57BL/6N female mice. Following surgery, mice were divided into the following four groups (n = 6 mice/group) as follows: sham, OVX control group, OVX + PTH (1–34) treated group (40 μg/kg/day), and OVX + dimeric ^{R25C}PTH treated group (40-80 μg/kg/day). OVX mice were allowed to recover for 4 weeks after surgery. Afterward, PTH (1–34) or ^{R25C}PTH was injected subcutaneously 5 times a week for 4 weeks. Micro-computed tomography (μ-CT) and histological analyses were performed on 4 groups at 18 weeks of age.'

We also appreciate the reviewer's helpful comment on histology analysis. We agree with the reviewer's comment that the primary spongiosa does not fully reflect bone remodeling. For histomorphometry analysis in young or male mice, we commonly use the secondary spongiosa, which more accurately reflects bone remodeling. However, in aged or OVX-induced osteoporosis mouse models, we use the primary and secondary spongiosa for histomorphometry analysis because of the barely detectable bone in the secondary spongiosa. In the TRAP staining, we observed an inhibitory effect of PTH on the osteoclast surface/bone surface, which was due to an increased bone surface in the PTH treatment group and less bone in the OVX-vehicle group. Serum CTX1 levels showed no significant difference between the OVX+vehicle and OVX+PTH(1-34) groups. We revised the Materials and Methods (page 21, line 502) and Discussion (page 14, line 330) sections as follows.

- 'In the histomorphometry analysis for TRAP staining, we used the secondary and primary spongiosa for the trabecular ROI because of the barely detectable in the secondary spongiosa of OVX model.'

- 'This study has several limitations. First, it is urgently necessary to determine whether dimeric ^{R25C}PTH is present in human patient serum. Second, TRAP staining showed an inhibitory effect of PTH treatment on the primary spongiosa area. However, the secondary spongiosa, which more accurately reflects bone remodeling (55), was not examined due to the barely detectable bone in this area in OVX-induced osteoporosis mouse models. Third, it is unclear whether similar bone phenotypes exist between human ^{R25C}PTH patients and dimeric ^{R25C}PTH-treated mice, particularly regarding low bone strength. Although the dimeric ^{R25C}PTH-treated group showed higher cortical BMD compared to WT-Sham or PTH groups, there was no difference in bone strength compared to the osteoporotic mouse model. Fourth, our study showed that PTH or ^{R25C}PTH treatment decreased circumferential length; it is uncertain if this phenotype is also present in PTH-treated or ^{R25C}PTH patients. Finally, we did not analyze the ^{R25C}PTH mutant mouse model, which would allow us to compare phenotypes that most closely resemble those of human patients.'

> *(2) It is also somewhat concerning that the age range is from 8-10 weeks, increasing the variability within the model. Did the age of mice differ between the groups analysed?*

We utilized mice of the same age (10 weeks) across all experiments involving the surgically induced ovariectomy (OVX) model described as above.

> *(3) Methods are not sufficiently detailed. For example, the regions used for histomorphometry are not described, there is no information on micro-CT thresholds, no*

> *detail on the force used for mechanical testing. Please address this request.*

Thank you for your comment. Let me address your points step by step.

(1) Thresholds for analysis were determined manually based on grayscale values for each experimental group as follows: trabecular bone: 3000; cortical bone: 5000 for all samples. We utilized an HA (calcium hydroxyapatite) phantom with HA content ranging from 0 to 1200 mg CaHA/cm³ to measure the grayscale values via μ-CT. These measurements were then used to generate a standard curve.

Author response image 1.

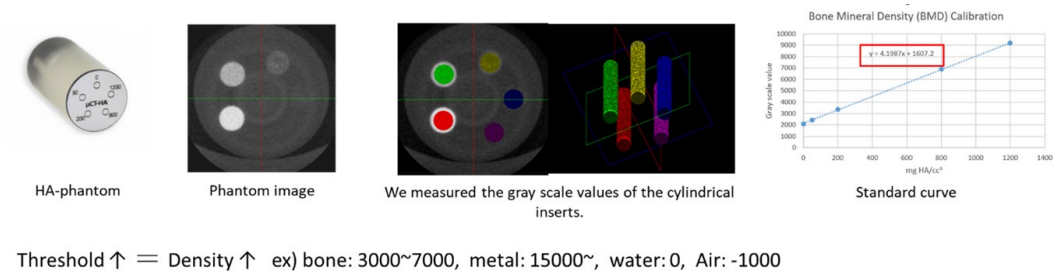

(2) Bone parameters and density were analyzed in the region between 0.3–1.755 mm (Voxel size: 9.7um, 150 slices) from the bottom of the growth plate. Analysis of bone structure was performed using adaptive thresholding in a CT Analyser.

Author response image 2.

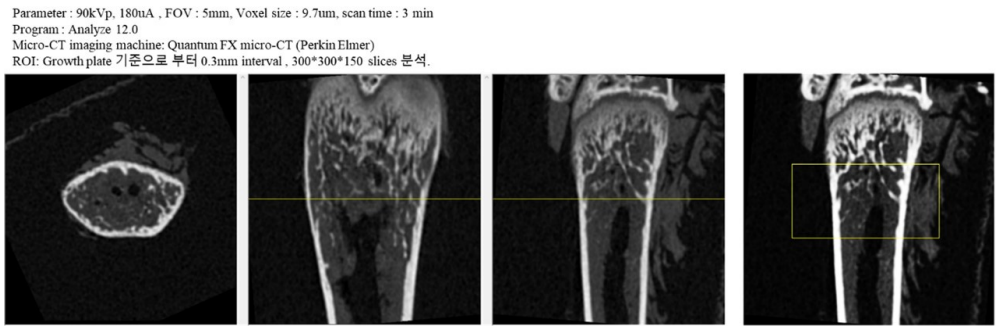

(3) Three-point bending test, the left femur of the mouse was immersed in 0.9 % NaCl solution, wrapped in gauze, and stored at −20°C until ready for a three-point bending test. In this test, we placed the mouse femurs positioned horizontally with the anterior surface facing upwards, centered on the supports, and the compressive force was applied vertically to the mid-shaft. The pressure sensor was positioned at a distance that allowed for the maximum allowable pressure (200N) without interfering with the test (20.0 mm for the femur). A miniature material testing machine (Instron, MA, USA) was used for this test. The crosshead speed was decreased to 1 mm/min until failure. During the test, force-displacement data were collected to determine the maximum load and slope of the bones.

(4) As the reviewer's suggestion, we revised the methods on page 20, line 477 and line 482-486 as follows.

- 'Bone parameters and density were analyzed in the region between 0.3–1.755 mm (150 slices) from the bottom of the growth plate. Analysis of bone structure was performed using adaptive thresholding in a μ-CT Analyser. Thresholds for analysis were determined manually

based on grayscale values for each experimental group: trabecular bone: 3000; cortical bone: 5000 for all samples.'

- 'The left femur of the mouse was immersed in 0.9 % NaCl solution, wrapped in gauze, and stored at −20°C until ready for a three-point bending test. In this test, we placed the mouse femurs horizontally with the anterior surface facing upwards, centered on the supports, and the compressive force was applied vertically to the mid-shaft. The pressure sensor was positioned at a distance that allowed maximum allowable pressure (1000N) without interfering with the test (20.0 mm for the femur). A miniature material testing machine (Instron, MA, U.S.A.) was used for this test. The crosshead speed was decreased to 1 mm/min until failure. During the test, force-displacement data were collected to determine the maximum load and slope of the bones.'

> *(4) There are three things unclear about the calvarial injection mouse model. Firstly, were the mice injected over the calvariae or with a standard subcutaneous injection (e.g. at the back of the neck)? If they were injected over the calvaria, why were both surfaces measured? Secondly, why was the dose of the R25C-PTH double that of PTH(1-34)? Thirdly, there is no justification for the use of "more intense coloration" as a marker of new bone; this requires calcein labelling to prove it new bone. It would be more reliable to measure and report the thickness of the calvaria. Please address these technical questions.*

Thank you for your valuable feedback on the calvarial injection mouse model. Below are our responses to the specific points mentioned:

(1) Injection method and measurement sites: The injections were administered subcutaneously above the calvaria, rather than at the standard subcutaneous site such as the back of the neck. This approach was chosen to ensure direct delivery of the peptide to the target area, enhancing the localized effects on bone formation. Measurements were taken at two different parts of the calvaria to account for any variation in the spread and absorption of the administered substance following injection. By analyzing both surfaces, we aimed to provide a comprehensive assessment of the impact on calvarial bone thickness.

(2) Dose of ^{R25C}PTH compared to PTH(1-34): The dose of ^{R25C}PTH used in our study was determined based on molecular weight calculations. The molecular weight of the dimeric ^{R25C}PTH(1-34) is approximately twice that of the monomeric PTH(1-34). Therefore, to maintain a consistent molar concentration and ensure comparable biological effects, the dose of ^{R25C}PTH was adjusted accordingly.

(3) Use of "more intense coloration" as a marker of new bone: We acknowledge that calcein labeling would provide a more reliable and quantifiable way to identify new bone formation. The use of “more intense coloration” was intended as a qualitative indicator in this study, and we recognize the technical limitations of this approach.

> *(5) The presentation of mechanical testing data is not sufficient. Example curves should be shown, and data corrected for bone size needs to be shown. The difference in mechanical behaviour is interesting, but does it stem from a difference in the amount of bone, or two a difference in the quality of the bone? Please explain this matter better in the manuscript.*

Thank you for your comment.

As a reviewer's comment, we provided example curves for the rat femur three-point bending test as shown below.

Author response image 3.

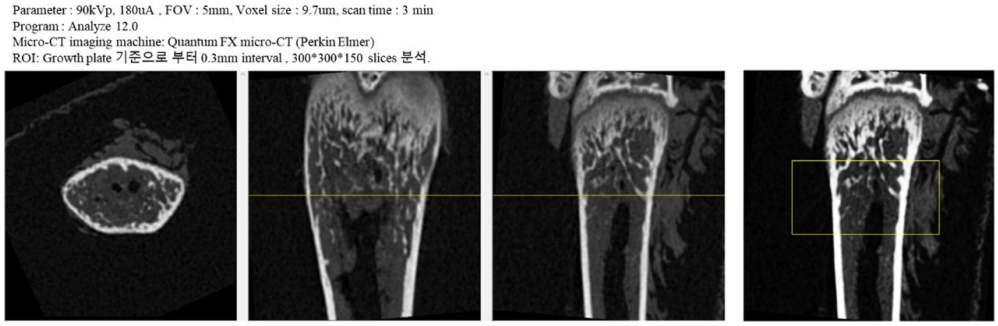

(1) The cortical bone area was decreased in the OVX-Vehicle and OVX-^{R25C}PTH(1-34) groups but not in the OVX-PTH(1-34) group compared to the Sham group. However, the total bone area was decreased in the PTH(1-34) and ^{R25C}PTH(1-34) treated groups, with no significant difference in the OVX-Vehicle group compared to the Sham group. Collectively, there was an increase in cortical thickness which resulted in a narrowing of the bone marrow space in OVX-^{R25C}PTH(1-34) groups. Accordingly, we revised Fig 5B with the addition of Tt.Ar and Ct.Ar.

(2) As the reviewer's suggestion, we revised the results on page 10, line 220-228 s follows.

- 'Quantitative micro-computed tomography (μ-CT) analysis of the femurs obtained from each group revealed that, as compared to OVX + vehicle controls, treatment with PTH(1–34) increased femoral trabecular bone volume fraction (Tb.BV/TV) by 121%, cortical bone volume fraction (Ct.BV/TV) by 128%, cortical thickness (Ct.Th) by 115%, cortical area (Ct.Ar) by 110%, and cortical area fraction (Ct.Ar/Tt.Ar) by 118% while decreased total tissue area (Tt.Ar) by 93% (Figure 5A and 5B). Treatment with dimeric ^{R25C}PTH(1-34) had similar effects on the femoral cortical bone parameters, as it increased Ct.BMD by 104%, Ct.BV/TV by 125%, Ct.Th by 107%, and Ct.Ar/Tt.Ar by 116%, while decreased Tt.Ar 86% (Figure 5). Considering the reduction of Tt.Ar and no change of Ct.Ar compared to the OVX+vehicle controls, the increase of Ct.Ar/Tt.Ar indicates a decrease in bone marrow space. The increase in cortical bone BMD was significant with dimeric ^{R25C}PTH(1-34) but not with PTH(1-34), whereas an increase in femoral trabecular bone was only observed with PTH(1-34).'

> *(6) The micro-CT analysis of the cortical bone in the OVX model is insufficient. Please indicate whether cross-sectional area has increased. Is there an increase in the size of the bones, or is the increase in cortical thickness due to a narrowing of the marrow space? This may help resolve the apparent contradiction between the cortical thickness data (where there is no difference between the two PTH formulations) and the mechanical testing data (where there is a difference). Please explain this matter better in the manuscript.*

Thank you for your comment.

(1) The cortical bone area was decreased in the OVX-Vehicle and OVX-^{R25C}PTH(1-34) groups but not in the OVX-PTH(1-34) group compared to the Sham group. However, the total bone area was decreased in the PTH(1-34) and ^{R25C}PTH(1-34) treated groups, with no significant difference in the OVX-vehicle group compared to the Sham group. Taken together, there was an increase in cortical thickness due to a narrowing of the bone marrow space in OVX-^{R25C}PTH(1-34) groups. Therefore, we revised as above.

(2) As the reviewer's suggestion, we revised the results on page 10, line 220-228 as follows.

- ‘Quantitative micro-computed tomography (μ-CT) analysis of the femurs obtained from each group revealed that, as compared to OVX + vehicle controls, treatment with PTH(1–34) increased femoral trabecular bone volume fraction (Tb.BV/TV) by 121%, cortical bone volume fraction (Ct.BV/TV) by 128%, cortical thickness (Ct.Th) by 115%, cortical area (Ct.Ar) by 110%, and cortical area fraction (Ct.Ar/Tt.Ar) by 118% while decreased total tissue area (Tt.Ar) by 93% (Figure 5A and 5B). Treatment with dimeric ^{R25C}PTH(1-34) had similar effects on the femoral cortical bone parameters, as it increased Ct.BMD by 104%, Ct.BV/TV by 125%, Ct.Th by 107%, and Ct.Ar/Tt.Ar by 116%, while decreased Tt.Ar 86% (Figure 5B). Considering the reduction of Tt.Ar and no change of Ct.Ar compared to the OVX+vehicle controls, the increase of Ct.Ar/Tt.Ar indicates a decrease in bone marrow space. The increase in cortical bone BMD was significant with dimeric ^{R25C}PTH(1-34) but not with PTH(1-34), whereas an increase in femoral trabecular bone was only observed with PTH(1-34).’

> *(7) The evidence that dimeric PTH has a different effect to monomeric PTH is very slim; I am not sure this is a real effect. Such differences take a long time to sort out (e.g. the field is still trying to determine whether teriparatide and abaloparatide are different). I think the authors need to look more carefully at their data - almost all effects are the same. Ultimately, the statement that dimeric PTH may be a more effective anabolic therapy than monomeric PTH are not supported by the data, and this should be removed. There is little to no difference found between normal PTH and the variant in their effects on calcium and phosphate homeostasis or on bone mass. However, the analysis has been somewhat cursory, with insufficient mechanical testing or cortical data presented. Many of the effects seem to be the same (e.g. cortical thickness, P1NP, ALP, vertebral BV/TV and MAR), but the way it is written it sounds like there is a difference. Please remove some of the unfounded claims that you have made in this manuscript.*

Thank you for your insightful comments. We strongly agree with your conclusion that PTH and dimeric ^{R25C}PTH indeed exhibit similar activities. We have toned-down our statement, however, there are still some elements showing statistical significance that need to be clearly stated. Specifically, when we changed the statistical method from *t*-test to one-way ANOVA, the significance of bone formation markers were only observed in dimeric PTH treated samples, and we have revised the manuscript of Results section on page 9, line 206-212 as follows to reflect the change.

- ‘These analyses revealed that both PTH(1-34) and dimeric ^{R25C}PTH(1-34) significantly increased the width of the new bone area by approximately four-fold, as compared to the vehicle group (Figure 4B). These findings thus support a capacity of dimeric ^{R25C}PTH(1-34) to induce new bone formation *in vivo,* similar to PTH, despite molecular and structural changes.’

Although it is unclear whether ^{R25C}PTH circulate as dimeric form or mutant monomeric form, the absence of bone resorption associated with long-term PTH exposure in the patients suggests the potential for a bone anabolic drug without side effects. Also, continued observation of the recently reported young patient in Denmark is expected to clarify this effect further. However, we acknowledge that our current data alone are insufficient to claim that ^{R25C}PTH may be a more effective anabolic therapy than wild type PTH, and we have adjusted our tone accordingly.

> *(8) Statistical analysis used multiple t-tests. ANOVA would be more appropriate.*

We agree with your suggestion. To compare the means among three or more groups, ANOVA is more appropriate than the *t*-test. Accordingly, we performed new statistical analyses using one-way and two-way ANOVA. One-way ANOVA was applied to figure 4, 5, and 6 (In previous, figure 5, 6, and 7), and two-way ANOVA was applied to Figure 3, considering both time and

treatment variables. We revised some of the figures and descriptions to reflect the changes in significance.

Thank you for Reviewer #1's thorough and thoughtful review. We greatly appreciate the suggestions and will incorporate them to enhance the quality of our paper.

> ***Reviewer #2 (Public Review):***
>
> *Summary:*
>
> *The study conducted by Noh et al. investigated the effects of parathyroid hormone (PTH) and a dimeric PTH peptide on bone formation and serum biochemistry in ovariectomized mice as a model for postmenopausal osteoporosis. The authors claimed that the dimeric PTH peptide has pharmacological benefits over PTH in promoting bone formation, despite both molecules having similar effects on bone formation and serum Ca2+. However, after careful evaluation, I am not convinced that this manuscript adds a significant contribution to the literature on bone and mineral research.*
>
> *Strengths:*
>
> *Experiments are well performed, but strengths are limited to the methodology used to evaluate bone formation and serum biochemical analysis.*
>
> *Weaknesses:*
>
> *(1) Limited significance of this study:*
>
> *• This study follows a previous study (not cited) reporting the effect of the dimeric R25CPTH(1-34) on bone regeneration in an osteoporotic dog (Beagle) model (Jeong-Oh Shin et al., eLife 13:RP93830, 2024). It's unclear why the authors tested the dimeric R25C-PTH peptide on a rodent animal model, which has limitations because the healing mechanism of human bone is more similar in dogs than in mice.*

Thank you for your interest in our research. To address the paper by Shin et al. (2024, DOI:10.7554/eLife.93830.1), we would like to clarify that our research on dimeric ^{R25C}PTH(1-34) was conducted first. Initially, we confirmed dimerization under *in vitro* conditions and observed its effects in a mouse model. Recognizing the need for additional animal models, we collaborated with Shin et al.'s team. Due to delays during the submission process, our paper was submitted later, which seems to have led to this misunderstanding. However, Shin et al. (2024) cited our pre-print article on bioRxiv (Noh, M., Che, X., Jin, X., Lee, D. K., Kim, H. J., Park, D. R., ... & Lee, S. (2024). Dimeric R25CPTH (1-34) Activates the Parathyroid Hormone-1 Receptor in vitro and Stimulates Bone Formation in Osteoporotic Female Mice. bioRxiv, 2024-03.DOI: 10.1101/2024.03.13.584815). Both Shin et al., and our mouse work supports the action of dimeric R25CPTH(1-34) on regulating bone metabolism.

> *• The authors should clarify why they tested the effects of dimeric ^{R25C}PTH(1-34) and not dimeric ^{R25C}PTH(1-84)?*

Thank you for your valid comments. Here are several reasons why we used the 1-34 fragment peptide in our experiment. Currently, PTH analog peptides for medical purposes include human parathyroid hormone fragment 1-34 (PTH(1-34)) and full-length recombinant human parathyroid hormone (rhPTH(1-84)). PTH(1-34) is used as a bone anabolic agent, while rhPTH(1-84) is used for PTH replacement therapy in hypoparathyroid patients with hypocalcemia. We aimed to compare the bone formation effects of R25CPTH with wild-type PTH, for which PTH(1-34) was deemed more appropriate. Additionally, previous studies have shown that both PTH(1-34) and PTH(1-84) possess equal ligand binding affinity for the PTH1 receptor. Key sites within the first 34 N-terminal amino acids of PTH are critical for high-

affinity interactions and receptor activation. Alterations in the N-terminal sequence of PTH(1-84) significantly reduce receptor binding, while truncations at the C-terminal end do not affect receptor affinity. The peptide used in our experiment was synthetic, and if the length does not affect affinity to its receptor affinity, the shorter length of PTH(1-34) made its synthesis more reasonable. Consequently, we tested the effects of PTH(1-34) and dimeric R25CPTH(1-34) due to its known efficacy on bone anabolic effect and relevance in receptor interactions. However, we aim to conduct functional analysis of the dimeric R25CPTH(1-84) in further study.

> *• The study is descriptive with no mechanism.*

We recognize that your concern is legitimate. While our study includes descriptive elements, it extends beyond mere observation. The R25CPTH research, which began with a case report, has evolved to utilize molecular techniques to better understand the unique physiological phenomena observed in patients. We have validated the peptide's dimerization caused by mutations *in vitro* and assessed their effects in both *in vitro* cell line models and *in vivo* mouse models. Although we have not yet confirmed whether ^{R25C}PTH exists as a dimer or monomer in patient blood, we anticipate it may exist in dimeric form at least some fractions and are currently conducting mass spectrometry on patient blood samples to determine this. Therefore, this paper serves as the first report on this PTH mutant suggesting that it may form a homodimer. Importantly, we are actively investigating the molecular mechanisms and downstream signaling pathways that differentiate normal PTH from dimeric ^{R25C}PTH. This includes analyzing differences in proteome and transcriptome induced by PTH and dimeric ^{R25C}PTH and examining the direct molecular characteristics and structural changes responsible for these mutations. Through this comprehensive approach, we aim to provide a detailed mechanistic understanding of ^{R25C}PTH in the subsequent publication.

> *(2) Statistics are inadequately described or performed for the experimental design:*
>
> *• The statistical analysis in Figure 5 needs to be written in a way that makes it clearer how statistics were done; t-test or one-way ANOVA?*

Sorry for the inconvenience and thank you for your thorough review. Initially, we conducted the statistical analysis using a t-test. However, during the revision process, we performed a new statistical analysis using one-way ANOVA, as it is more appropriate for comparing the means among three or more groups. Despite this change, there were no differences in statistical significance, so the descriptions remained unchanged.

> *• Statistics in Figures 6 and 7 should be performed by one-way ANOVA to compare the mean values of one variable among three or more groups, and not t-test.*

Thank you for your thorough review, and I apologize for any inconvenience. I agree with your suggestion that ANOVA is more appropriate than the t-test for comparing means among three or more groups. Accordingly, we performed new statistical analyses using one-way ANOVA. When we changed the statistical method from t-test to one-way ANOVA, the significance of bone formation markers, P1NP and ALP, appeared only in dimeric R25CPTH and not in wild-type PTH. We have reflected these findings in the text.

> *(3) Misleading and confused discussion:*
>
> *• The first paragraph lacks clarity in the PTH nomenclature and the authors should provide a clear statement that the PTH mutant found in patients is likely a monomeric R25CPTH(1-84), considering that there has been no proof of a dimeric form.*

Thank you for your insightful comments. I agree that there was some ambiguity in the nomenclature used in the first paragraph of the Discussion section. However, we do not believe that no proof of a dimeric form of the ^{R25C}PTH(1-84) mutant necessarily indicates that the PTH mutant in the blood is solely monomeric. Identifying the *in vivo* structure of ^{R25C}PTH(1-84) is one of the goals of our ongoing project. While the exact form of ^{R25C}PTH(1-84) in patients is still elusive, we are investigating the possibility that some fraction may exist as a dimer. On page 12, line 274-276, we have revised the content to address this issue and improve clarity as follows.

- 'In this study, we show the introduction of a cysteine mutation at the 25th amino acid position of mature parathyroid hormone (^{R25C}PTH) facilitates the formation of homodimers comprised of the resulting dimeric R25CPTH peptide *in vitro*.'

> *• Moreover, the authors should discuss the study by White et al. (PNAS 2019), which shows that there are defective PTH1R signaling responses to monomeric R25CPTH(1-34). This results in faster ligand dissociation, rapid receptor recycling, a short cAMP time course, and a loss of calcium ion allosteric effect.*

Sorry for the inconvenience and thank you for your thorough review. The authors were aware of the referenced paper and deeply apologize for its omission during the writing and editing process. Citing this paper will enhance the credibility of our findings. We have now included this citation and made the necessary adjustments to the manuscript of Discussion section on page 12, line 295-296 as follows.

- 'We also observed that the potency of cAMP production in cells was lower for dimeric ^{R25C}PTH as compared to the monomeric ^{R25C}PTH, in accordance with a lower PTH1R-binding affinity. Previous reports indicated that a mutation at the 25th position of PTH results in the loss of calcium ion allosteric effects on monomeric ^{R25C}PTH, leading to faster ligand dissociation, rapid receptor recycling, and a shorter cAMP time course (50). Correspondingly, the weaker receptor affinity and reduced cAMP production observed in dimeric ^{R25C}PTH suggest a possibility that the formation of a disulfide bond at the 25th position significantly alters the function of PTH as a PTH1R ligand. These structural effects are not yet fully understood and need to be investigated further.'

> *• The authors should also clarify what they mean by "the dimeric form of R25CPTH can serve as a new peptide ...(lines 328-329)" The dimeric R25CPTH(1-34) induces similar bone anabolic effects and calcemic responses to PTH(1-34), so it is unclear what the new benefit of the dimeric PTH is.*

We apologize for any confusion in our previous description. We concur that, as you mentioned, PTH and dimeric ^{R25C}PTH indeed exhibit similar activities. We have toned-down our statement, however, there are still some elements showing statistical significance that need to be clearly stated. Specifically, when we changed the statistical method from *t*-test to one-way ANOVA, the significance of bone formation markers was only observed in dimeric PTH treated samples, and we have revised the manuscript of Results section on page 9, line 206-212 as follows to reflect the change.

- 'These analyses revealed that both PTH(1-34) and dimeric ^{R25C}PTH(1-34) significantly increased the width of the new bone area by approximately four-fold, as compared to the vehicle group (Figure 4B). These findings thus support a capacity of dimeric ^{R25C}PTH(1-34) to induce new bone formation *in vivo*, similar to PTH, despite molecular and structural changes.'

Although it is unclear whether ^{R25C}PTH circulate as dimeric form or mutant monomeric form, the absence of bone resorption associated with long-term PTH exposure in the patients

suggests the potential for a bone anabolic drug without side effects. Also, continued observation of the recently reported young patient in Denmark is expected to clarify this effect further. However, we acknowledge that our current data alone are insufficient to claim that ^{R25C}PTH may be a more effective anabolic therapy than wild type PTH, and we have adjusted our tone accordingly.

Thank you for Reviewer #2's comprehensive and considerate review. We are grateful for the ideas, and we have revised our manuscript accordingly them to improve our paper.

> ***Reviewer #1 (Recommendations For The Authors):***
>
> *(1) Figure 1D lacks molecular weight markers.*

Thank you for your thorough review. We added protein molecular weight markers in the figure.

> *(2) The lack of change in plasma cAMP is very surprising, particularly given that there is no difference in the effect of the two forms of PTH on serum calcium or phosphate, or urinary phosphate. This data is somewhat of a distraction since no effort has been made to assess the difference in the effects of these PTH forms on kidney function. I suggest removing this data and spending time working on the origin of this difference.*

Thank you for your insightful comments and valuable suggestions on our manuscript. We also could not precisely explain the discrepancy between the cell line and animal model experiments. However, since the results were consistently observed, we included them in the paper as they may be significant. We acknowledge that in the context of our current research, these data lack sufficient correlation with other findings. Therefore, we have removed the data about the lack of change in plasma cAMP by PTH injection (Figure 4. Effect of cAMP production by PTH injection in CD1 female mice) and revised the manuscript accordingly (Page 8, line 188-194; page 12, line 301-306; page 19, line 454-456). We are currently conducting further research with multiomics data analysis to elucidate potential differences in the sub-signaling pathways between PTH and dimeric R25CPTH, to identify the specific functions affected by these variations, and to understand the underlying mechanisms. The lack of changes in plasma cAMP levels *in vivo* will be addressed in a subsequent publication detailing our findings.

> *(3) Introduction, line 61. The authors state that "most" anti-resorptive therapies cannot stimulate new bone formation. I don't believe that ANY anti-resorptive therapies stimulate new bone formation! If there is one, this should be referenced.*

Thank you for pointing out important aspects. Romosozumab, a humanized monoclonal anti-sclerostin antibody, has a dual effect by enhancing bone formation and inhibiting bone resorption. Sclerostin, a protein produced by osteocytes, plays a role in the regulation of bone metabolism. It promotes osteoclast differentiation, which is associated with bone resorption, and suppresses osteoblast activity, which is crucial for bone formation. By binding to sclerostin, Romosozumab prevents it from blocking the signaling pathways necessary for osteogenesis. Consequently, Romosozumab therapy not only regulates bone resorption but also affects new bone formation. We added the references to that information.

> *(4) The authors tend to include a lot of methods in the results section (e.g. describing the number of replicates, and details of histological analysis). This should be minimized.*

Thank you for your thorough review, and sorry for the inconvenience. We have minimized the methodological details in the results section, ensuring that only essential information for understanding the findings and the procedures remain.

> *(5) Lines 302-305: If retaining the blood cAMP data, please provide references for the assertion that renal PTH receptors mediate this response.*

PTH exerts its effects primarily through the PTH1 receptor (PTH1R), a G protein-coupled receptor present in various tissues, including bone and kidney (Chase et al., 1968, Chase et al., 1970). When activated by PTH, this receptor stimulates the production of cyclic AMP (cAMP), with the kidneys playing a significant role in this process (Maeda et al., 2013). In the initial manuscript, the importance of renal PTH receptors in mediating the blood cAMP response may have been overemphasized. We appreciate your feedback on this point, and we have provided references to support this assertion. However, by process following the former 'Recommendations for the Authors', we removed the data about the lack of change in plasma cAMP by PTH injection, the description of the renal PTH receptors mediate this response of blood cAMP also removed.

- Chase, Lewis R., and G. D. Aurbach. "Renal adenyl cyclase: anatomically separate sites for parathyroid hormone and vasopressin." Science 159.3814 (1968): 545-547.DOI:10.1126/science.159.3814.545

- Chase, Lewis R., and G. D. Aurbach. "The effect of parathyroid hormone on the concentration of adenosine 3', 5'-monophosphate in skeletal tissue in vitro." Journal of Biological Chemistry 245.7 (1970): 1520-1526.DOI:10.1016/S0021-9258(19)77126-9

- Maeda, Akira, et al. "Critical role of parathyroid hormone (PTH) receptor-1 phosphorylation in regulating acute responses to PTH." Proceedings of the National Academy of Sciences 110.15 (2013): 5864-5869.DOI: 10.1073/pnas.1301674110

> *(6) Eosin stains bone pink and haematoxylin stains cells purple. This has been incorrectly described in the manuscript.*

Thank you for your thorough review, and I apologize for any confusion caused by the poor description. It appears that the terms were used interchangeably during the editing process. We have corrected the description in the manuscript and will ensure such mistakes do not occur again in the future.

> *(7) Sodium thiosulphate is a fixative for Von Kossa staining, not an agent that removes nonspecific binding.*

Thank you for your careful review. However, there seems to be a misunderstanding of sodium formaldehyde as sodium thiosulfate. A 5% sodium thiosulfate solution is a critical in vitro diagnostic agent used in various staining kits. As a reducing agent, it effectively removes excess silver ions in staining kits based on silver impregnation techniques. In our experiment, sodium thiosulfate was specifically used to remove residual silver ions in Von Kossa staining. For more details, please refer to the following link: https://www.morphisto.de/en/shop/detail/d/Natriumthiosulfat_5//12825/.

> ***Reviewer #2 (Recommendations For The Authors):***
>
> *Moderate-to-Minor points:*
>
> *• Line 73: it's either class B GPCR or secretin receptor family but not class B GPCR family.*

Thank you for your thorough review, and I apologize for any confusion in our previous description. We corrected the description in the manuscript as class B GPCR.

> *• Line 79: correct "adenylate cyclase" to "transmembrane adenylate cyclases"*

Thank you for your thorough review, and I apologize for any confusion in our previous description. We corrected the description in the manuscript as transmembrane adenylate cyclases.

> *• Line 89: should "hypothyroidism" be "hypoparathyroidism"?*

Thank you for your thorough review, and I apologize for any confusion in our previous description. We corrected the description in the manuscript as hypoparathyroidism.

> *• Line 159: all agonists display higher binding affinities when their receptors are coupled to G proteins, so it's unclear why the higher affinity of the dimeric ^{R25C}PTH(1-34) for the RG state seems to be important for the authors.*

Thank you for your insightful comments. First of all, comparing the binding affinities of the R0 (G protein-uncoupled) and RG (G protein-coupled) conformations of the receptor is inappropriate. This is because the form and size of the radio-label ligand bound to each conformation differ, which consequently affects their binding affinities and, in turn, influences the binding strength of target ligands such as PTH, monomeric ^{R25C}PTH, and dimeric ^{R25C}PTH. Therefore, it is preferable to compare how the binding strengths of test ligands differ for each conformation. Additionally, the fact that significant binding affinity is lost for R^0 while remaining high for the RG conformation of PTH1R is important because typical PTH exhibits high binding affinity for R0, whereas PTHrP shows higher affinity for the RG conformation. This suggests that dimeric ^{R25C}PTH may possess distinct molecular characteristics and potentially induce different downstream signaling pathways compared to typical PTH.

> *• Line 169-170 and Fig. 2: According to the theory of receptor pharmacology established in the 60s' for native receptors (Arch. Int. Pharmacodyn. 127:459-478 (1960); Arch. Int. Pharmacodyn. 136:385-413 (1962)) and verified later in the 80-90's for recombinant GPCRs, the activity constant (Kact or EC50) value of hormone actions in various tissues or cells is equal to the dissociation constant (Kd) of the hormone when receptors are not overexpressed (EC50 = Kd). When receptors are overexpressed (presence of spare receptors), then EC50 < Kd. Assuming that after Cheng-Prussof correction for data in Fig. 2, IC50 < Ki = Kd, how do the authors explain that IC50 values for RG are about 1-Log lower than EC50s (i.e., EC50 > Kd)?*

We appreciate your insightful comment and fully acknowledge the established theory of receptor pharmacology, which states that Kd equals EC50, and when the receptor is overexpressed, EC50 is less than Kd. After having read your comments, we have revisited this paper Okazaki et al, PNAS, 2008 to better understand the PTH interaction with PTH1R. While our data might appear to contradict this theory, we believe that a direct comparison between the IC50 of RG and the EC50 in Figure 2 may not be entirely appropriate for the following reasons. First, the IC50 was determined from membrane preparations of a receptor-overexpressing cell line (GP-2.3), whereas the EC50 was calculated based on the cAMP response in SaOS-2 cells. These different experimental conditions contribute to the observed discrepancies. Second, the peptides used in the competition assays differ. R^0 utilized radiolabeled PTH(1-34), while RG employed M-PTH(1-15) with several amino acid substitutions and a shorter length. This further complicates a direct comparison between the EC50 and IC50 values in our study.

Thank you for all the reviewers' thorough and thoughtful reviews. We greatly appreciate your suggestions and have addressed all the issues to enhance the quality of our paper.

https://doi.org/10.7554/eLife.97579.2.sa0